Schweizerische Eidgenossenschaft
Confédération suisse
Confederazione Svizzera
Confederaziun svizra

Federal Department of the Environment, Transport, Energy and Communications DETEC

Swiss Federal Office of Energy SFOE
Energy Research and Cleantech Division

Final report dated 08.09.2022

High Performance Sodium-Nickel Chloride Cell (HiPerSoNick)

Cella Sodio Cloruro di Nichel ad elevata prestazione (HiPerSoNick)

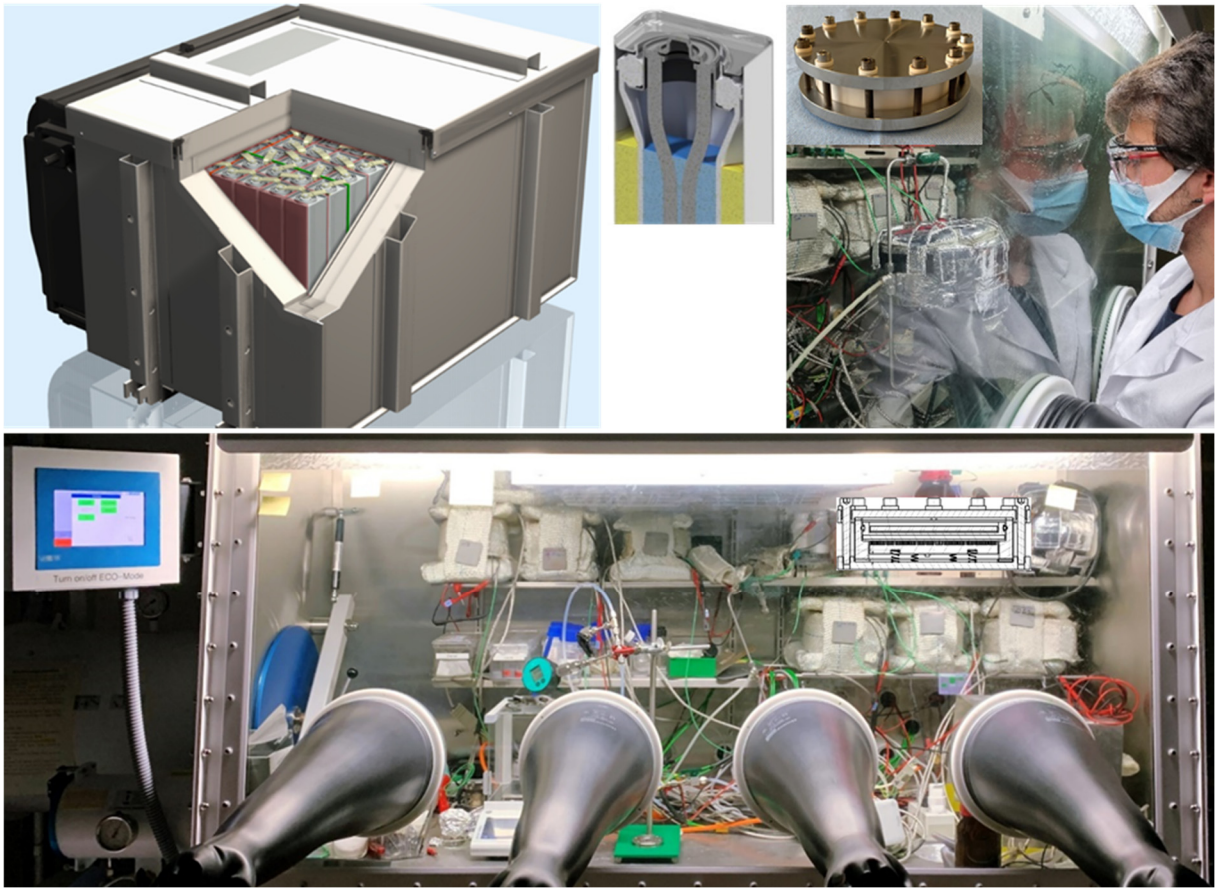

Source: ©FZSoNick,Empa 2022

Date: 08.09.2022

Location: Bern

Publisher:
Swiss Federal Office of Energy SFOE
Energy Research and Cleantech
CH-3003 Bern
www.bfe.admin.ch

Subsidy recipients:

Empa
Überlandstrasse 129
CH-8600 Dübendorf
www.empa.ch/econversion

FZSoNick
Via Laveggio
CH-6855 Stabio
www.fzsonick.com

EPFL
Station 9
CH-1015 Lausanne
www.epfl.ch

Authors:

Meike Heinz,	**Empa**,	**meike.heinz@empa.ch**
Tu Lan,	Empa,	tu.lan@empa.ch
Enea Svaluto-Ferro,	Empa,	enea.svaluto-ferro@empa.ch
Corsin Battaglia,	Empa,	corsin.battaglia@empa.ch
Daniel Landmann,	Empa,	2018/07-2022/02
Gustav Graeber,	Empa,	2019/10-2021/02
Omar Pecho,	Empa,	2018/07-2019/06
Marie-Claude Bay,	Empa,	2019/01-2020/06
Natalia Kovalska,	Empa,	natalia.kovalska@empa.ch
Gurdial Blugan,	Empa,	gurdial.blugan@empa.ch
Thomas Graule,	Empa,	thomas.graule@empa.ch
Clark Ligon,	Empa,	2018/07-2020/03
Sophia Haussener,	EPFL,	sophia.haussener@epfl.ch
Ronald Gutierrez,	EPFL,	ronald.gutierrezperez@epfl.ch
Andrea Pozzi,	**FZSoNick**,	**andrea.pozzi@fzsonick.com**
Alberto Turconi,	FZSoNick,	alberto.turconi@fzsonick.com
Diego Basso,	FZSoNick,	diego.basso@fzsonick.com
Giuseppe Lodi,	FZSoNick,	2018/07-2021/11
Giorgio Crugnola,	FZSoNick,	2018/07-2018/12

SFOE project coordinators:
Men Wirz, men.wirz@bfe.admin.ch

SFOE contract number: SI/501674-01

The authors bear the entire responsibility for the content of this report and for the conclusions drawn therefrom.

Zusammenfassung

Das Projekt HiPerSoNick konzentrierte sich auf die Entwicklung von Zellen der nächsten Generation für Hochtemperatur-Natrium-Nickelchlorid-Batterien. Diese saubere, effiziente und sichere Technologie, die sich bereits als Lösung für Notstromanwendungen bewährt hat, leidet unter niedrigen Laderaten und begrenzter Leistungsdichte bei hohen Entladeströmen. Handelsübliche Natrium-Nickelchlorid-Zellen mit röhrenförmiger Geometrie haben eine Nennkapazität von 38-40 Ah bei einer aktiven Fläche von ~260 cm^2 (Kathodenbeladung ~150 mAh/cm^2). Die Zellen werden bei Temperaturen von etwa 300 °C betrieben und sind für den Dauerbetrieb bei hohen Entladestromdichten von 50 mA/cm^2 ausgelegt. Dies führt angesichts der hohen Kathodenbeladung zu relativ niedrigen Entladeraten von C/3. Außerdem sind die Produktionskosten der röhrenförmigen Hochtemperaturzellen im Vergleich zu Lithium-Ionen-Batterien relativ hoch. Die Kosten für Hochtemperatur-Natrium-Nickelchlorid-Batteriepacks belaufen sich derzeit auf 300-350 $/kWh, was bei einer Lebensdauer von 4500 Zyklen zu Gesamtenergiekosten von 0,07-0,08 $/kWh/Zyklus führt. Wie in diesem Projekt gezeigt wurde, können moderne röhrenförmige Zellen in Langzeit-Zyklusstudien Entladeenergien von ~350 Wh/kg bei C/3 liefern (relativ zur Kathodenmasse) .

Im Rahmen des HiPerSoNick-Projekts führten wir eine umfassende Ko-Entwicklung von Zelldesign, Elektrolyt, Dichtungsmitteln und Elektroden durch. Die beiden Hauptziele des Projekts waren **(i)** der Nachweis der Machbarkeit eines **planaren Zellendesigns** und **(ii)** die **Verringerung des Nickelgehalts** der Kathode, in beiden Fällen ohne Beeinträchtigung der Leistung und der Zykluslebensdauer der Batterie. Der Übergang von einem röhrenförmigen zu einem planaren Zellendesign birgt das Potenzial, die Produktionskosten zu senken, da planare Komponenten besser mit automatisierten Großserienfertigungen und Qualitätskontrollroutinen kompatibel sind. Die Entwicklung planarer Natrium-Nickel-Chlorid-Zellen steht seit mehr als 10 Jahren im Fokus der Forschung, aber frühere Studien beschränkten sich auf kleine Zellen (z. B. 3 cm^2 aktive Fläche) mit Schwerpunkt auf moderaten Kathodenbeladungen (50 mAh/cm^2) und niedrigen Stromdichten (10 mA/cm^2). In diesem Projekt haben wir zunächst eine vielseitige planare Prototyp-Zellenplattform mit ~3 cm^2 aktiver Fläche entwickelt. In symmetrischen Zellen demonstrierten wir das elektrochemische Abscheiden und Auflösen von geschmolzenem Natrium bei extrem hohen Stromdichten (bis zu 2600 mA/cm^2), ohne dass sich Natriummetalldendriten bildeten. In Vollzellen mit mäßiger Kathodenbeladung (50 mAh/cm^2) erreichten wir die höchste spezifische Entladeenergie, die bisher in der Literatur für längere Zyklen von planaren Hochtemperatur-Natrium-Nickelchlorid-Zellen berichtet wurde (277 Wh/kg für Standardkathoden, bestehend aus Nickel und Eisen, gemittelt über 50 Zyklen; Entladung bei 80 mA/cm^2, 1,6C). Wir haben eine Reihe von passiven Zellkomponenten entwickelt, um die (teilweise) geschmolzenen und korrosiven Materialien in den Zellen auch bei hohen Kathodenbelastungen zu handhaben. Zum ersten Mal erreichten wir einen stabilen Zyklus von modernen Nickel/Eisen-Kathoden bei einer Kathodenbeladung von 150 mAh/cm^2, was dem entspricht, was in kommerziellen Röhrenzellen verwendet wird. Bei solch hohen Kathodenbeladungen und Entladestromdichten von bis zu 80 mA/cm^2 (>C/2) konnten wir mehr als 50 stabile Zyklen nachweisen und gleichzeitig die Entladeenergie weiter steigern (auf >300 Wh/kg).

In einem nächsten Schritt haben wir die Prototypzellen auf größere Pilotzellen (~90 cm^2 aktive Fläche) skaliert. Um geeignete planare keramische Elektrolyte bereitzustellen, entwickelten wir skalierbare Formgebungs- und Sinterverfahren für Na-β"-Aluminiumoxid. Unser Projekt bietet zwei verschiedene erfolgreiche Verfahren, die entweder auf dem großflächigen Bandgießen und Laminieren oder dem Pressen von Na-β"-Aluminiumoxid mit anschließendem Sintern basieren und zu robusten planaren Na-β"-Aluminiumoxid-Elektrolytscheiben mit einer Fläche von ~95 cm^2 führen. Darüber hinaus untersuchten wir temperaturbeständige Glasdichtungen, die für die Langzeitstabilität planarer Zellen entscheidend sind, aber auch ein großes Potenzial für Kosteneinsparungen bei röhrenförmigen Zellen bieten. Wir

identifizierten geeignete Glasdichtungskandidaten für Keramik-Keramik- und Keramik-Metall-Verbindungen, die für die Zellmontage erforderlich sind. In Modellexperimenten konnten wir die Bedeutung der Dichtungsgeometrie und ihrer Verarbeitung nachweisen, mit der sich die geforderten niedrigen Leckraten erreichen lassen.

Um unsere Entwicklungen im Hinblick auf das Projektziel **(i)** zu demonstrieren, haben wir die erfolgreichsten **planaren Zellkomponenten** vom Prototyp auf Pilotzellen übertragen. Zum ersten Mal berichteten wir über elektrochemische Zyklen von planaren Hochtemperatur-Natrium-Nickelchlorid-Zellen mit einer großen aktiven Fläche von etwa 90 cm^2. Die besten Ergebnisse wurden bei einer Kathodenbeladung von 80 mAh/cm^2 erzielt, wobei eine kumulative Kapazität von 3,4 Ah/cm^2 über 2,5 Monate bei niedrigen Stromdichten (bis zu 10 mA/cm^2 beim Laden, bis zu 20 mA/cm^2 beim Entladen) erreicht wurde. Geometrische Variationen und Maßtoleranzen der Zellkomponenten, insbesondere der gesinterten Keramikteile, behindern jedoch eine präzise Anpassung, ein effizientes Management der geschmolzenen Materialien und eine hermetische Versiegelung der planaren Pilotzellen, wodurch die Zykluslebensdauer im derzeitigen Entwicklungsstadium beeinträchtigt wird. Darüber hinaus haben wir festgestellt, dass die passiven Komponenten, die entlang des Umfangs der planaren Zellen erforderlich sind, bei dieser Geometrie zu zusätzlichem Gewicht und Kosten führen. Während die Vorteile eines planaren Zelldesigns sicherlich Potenzial für eine groß angelegte Produktion bieten, müssen alternative Zellmaterialien und/oder Zellstapel eingesetzt werden, um eine Erhöhung des Zellgewichts zu vermeiden. Zum gegenwärtigen Zeitpunkt müssen solche Änderungen weiter untersucht werden, um die Anforderungen an Sicherheit und Lebensdauer kommerzieller Hochtemperaturbatterien zu erfüllen.

Da das Nickel in der Kathode wesentlich zu den Kosten und dem Gewicht von Natrium-Nickelchlorid-Zellen beiträgt, haben wir verbesserte Kathodenformulierungen mit **reduziertem Nickelgehalt** entwickelt. Durch die Einführung eines Kohlenstoffzusatzes und die Verbesserung der Verarbeitung konnten wir den Nickelgehalt um bis zu 20 Gew.-% (-25 g pro Zelle) reduzieren, was nicht nur die Kosten und das Gewicht der Kathode verringert, sondern auch ihre Leistung in Bezug auf Ladezeit, Entladeenergie und Zykluslebensdauer erhöht. Um unsere Entwicklungen im Hinblick auf das Projektziel **(ii)** zu demonstrieren, haben wir die verbesserten Kathodenformulierungen erfolgreich in Pilotzellen der nächsten Generation mit röhrenförmiger Geometrie integriert. Die Langzeitstabilität wurde durch Modultests an 10 Röhrenzellen jeder Zusammensetzung untersucht, wobei ein Lebensdauertestverfahren für bis zu 6 Monate angewandt wurde. Im Vergleich zu Kathoden nach dem Stand der Technik weisen die verbesserten Formulierungen geringere Ladezeiten und höhere Entladungsenergien bei Langzeitzyklen auf (z. B. 10,5 h gegenüber 12,0 h; 386 gegenüber 346 Wh/kg nach 200 Lebenszyklen, 4 Monate). Sie weisen auch eine geringere Degradationsrate auf und werden voraussichtlich nach fast 7000 Zyklen noch 80 % der Entladeleistung von Standardkathoden erreichen. Während also die Kostensenkungen durch die Verringerung des Nickelgehalts moderat ausfallen (z. B. -5 $/kWh bei einem Ni255-Preis von 20 €/kg), können durch die gleichzeitige Verlängerung der Zyklenlebensdauer die resultierenden Gesamtenergiekosten erheblich auf 0,04-0,05 $/kWh/Zyklus gesenkt werden. FZSoNick plant, die neu entwickelten Kathodenformulierungen mit reduziertem Nickelanteil ab Anfang 2023 in der Produktion seiner Batterien einzusetzen.

Unsere Entwicklungen sowohl an planaren als auch an röhrenförmigen Natrium-Nickelchlorid-Zellen in den letzten vier Jahren zeigen die Vorteile und Grenzen beider Geometrien. Planare Zellen bieten große Flexibilität, da sie Kathoden mit unterschiedlicher Kapazität und Packungsdichte sowie variable Stromabnehmer an Anode und Kathode integrieren können. Die Entwicklung planarer Hochtemperatur-Natrium-Nickelchlorid-Zellen im Rahmen des HiPerSoNick-Projekts bringt die Forschung und Entwicklung in diesem Bereich erheblich voran. Kommerzielle röhrenförmige Natrium-Nickelchlorid-Zellen bieten jedoch, bei gleicher Kathodenbelastung, nach wie vor einen geringeren Zellwiderstand und damit eine höhere Entladeenergie als derzeitige planare Zellen im Labormaßstab. Darüber hinaus konnte bisher noch nicht gezeigt werden, dass große planare Zellen (>3 cm^2) hermetisch verschlossen

werden können, so dass ein stabiler Langzeitbetrieb bei Betriebstemperaturen von ~300 °C in Umgebungsluft möglich ist. Weitere Entwicklungen sind erforderlich, um ihr Design zu verbessern, sowohl im Hinblick auf die Zykluslebensdauer, die Zellbeständigkeit, das Gewicht/Volumen der Zelle, die Zuverlässigkeit als auch die Kosteneffizienz. Röhrenzellen unterliegen einer Reihe von Beschränkungen, z. B. hinsichtlich des Volumens und der Packungsdichte des Kathodengranulats, bieten jedoch einen geringen Zellwiderstand und eine effiziente Langzeitzyklusdauer.

Basierend auf den im HiPerSonick-Projekt entwickelten Kompetenzen, sowohl in Bezug auf die planare Zellentwicklung als auch auf die Kathodenmodifikation, entwickeln Empa und FZSoNick derzeit im Horizon 2020-Nachfolgeprojekt "Sodium-zinc molten-salt batteries for low-cost stationary storage (SOLSTICE)" (www.solstice-battery.eu) alternative Kathodenformulierungen, bei denen Nickel durch kostengünstigeres Zink ersetzt wird.

Résumé

Le projet HiPerSoNick était axé sur le développement de cellules de nouvelle génération pour les batteries au sodium et chlorure de nickel à haute température. Déjà éprouvée pour les applications d'alimentation de secours, cette technologie propre, efficace et sûre souffre de faibles taux de charge et d'une limitation de la densité de puissance à des courants de décharge élevés. Les cellules au sodium et chlorure de nickel commerciales à géométrie tubulaire ont une capacité nominale de 38-40 Ah pour une surface active de ~260 cm^2 (charge de la cathode ~150 mAh/cm^2). Utilisées à des températures d'environ 300 °C, les cellules sont prévues pour un fonctionnement continu à des densités de courant de décharge élevées de 50 mA/cm^2. Cela se traduit par des taux de décharge relativement faibles de C/3, compte tenu de la capacité cathodique élevée. En outre, les coûts de production des cellules tubulaires à haute température sont relativement élevés, par rapport aux batteries lithium-ion. Les coûts des blocs de batteries au sodium et chlorure de nickel à haute température s'élèvent actuellement à 300-350 $/kWh, ce qui se traduit par des coûts énergétiques globaux de 0,07-0,08 $/kWh/cycle, en considérant une durée de vie nominale de 4500 cycles. Comme le montre ce projet, les cellules tubulaires de pointe peuvent fournir des énergies de décharge de ~350 Wh/kg dans les études de cyclage à long terme à C/3 (relatif à la masse cathodique).

Dans le cadre du projet HiPerSoNick, nous avons procédé à un co-développement complet de la conception des cellules, de l'électrolyte, des matériaux d'étanchéité et des électrodes. Les deux principaux objectifs du projet étaient **(i)** de démontrer la faisabilité d'une conception de **cellule plane**, et **(ii)** de **réduire la teneur en nickel** de la cathode, dans les deux cas sans compromettre les performances et la durée de vie de la batterie. Le passage d'un concept de cellule tubulaire à un concept de cellule plane présente un potentiel de réduction des coûts de production, car les composants planaires sont plus compatibles avec la fabrication automatisée à grand volume et les routines de contrôle de la qualité. Le développement de cellules planes au sodium et chlorure de nickel est au centre des préoccupations de la communauté des chercheurs depuis plus de 10 ans, mais les études précédentes étaient limitées à des cellules de petite taille (par exemple 3 cm^2 de surface active), avec une focalisation sur des charges cathodiques modérées (50 mAh/cm^2) et de faibles densités de courant (10 mA/cm^2). Dans ce projet, nous avons d'abord développé un prototype de cellule plane polyvalente avec une surface active de ~3 cm^2. A l'aide de cellules symétriques, nous avons démontré la dissolution et le dépôt électrochimiques de sodium fondu à des densités de courant extrêmement élevées (jusqu'à 2600 mA/cm^2), sans formation de dendrites de sodium métallique. A l'aide de cellules complètes avec une charge cathodique modérée (50 mAh/cm^2), nous avons atteint l'énergie de décharge spécifique la plus élevée (par rapport à la littérature existante) pour un cyclage prolongé de cellules planes à haute température au sodium et chlorure de nickel (277 Wh/kg pour des cathodes standard composées de nickel complété par du fer, moyenne sur 50 cycles ; décharge à 80 mA/cm^2, 1.6C). Nous avons également développé un certain nombre de composants passifs pour gérer les matériaux (partiellement) fondus et corrosifs dans les cellules, même à des charges cathodiques élevées. Pour la première fois, nous avons obtenu un cycle stable des cathodes nickel/fer de pointe à une charge cathodique de 150 mAh/cm^2, correspondant à ce qui est employé dans les cellules tubulaires commerciales. Avec des charges cathodiques aussi élevées et des densités de courant de décharge allant jusqu'à 80 mA/cm^2 (>C/2), nous avons pu démontrer plus de 50 cycles stables, tout en augmentant encore l'énergie de décharge (jusqu'à >300 Wh/kg).

Dans une étape suivante, nous avons adapté les cellules prototypes à des cellules pilotes plus grandes (~90 cm^2 de surface active). Pour fournir des électrolytes céramiques planaires appropriés, nous avons développé des procédures extensibles de mise en forme et de frittage pour la β''-alumine de sodium (Na-β''-Al_2O_3). Notre projet fournit deux procédures fonctionnelles différentes, basées soit sur le coulage en bande de grande surface et la stratification, soit sur le pressage de la β''-alumine de sodium suivi d'un frittage, ce qui permet d'obtenir des disques d'électrolyte plans robustes en β''-alumine de sodium d'une surface de ~95 cm^2. Nous avons également étudié les joints en verre thermorésistant, qui sont essentiels pour la stabilité à long terme des cellules planes, mais qui offrent également un grand potentiel de réduction des coûts dans les cellules tubulaires. Nous avons identifié des joints en verre appropriés pour les joints céramique-céramique et céramique-métal nécessaires à l'assemblage des cellules. Dans des expériences modèles, nous avons démontré l'importance de la géométrie du joint et de son traitement, qui permet d'atteindre les faibles taux de fuite requis.

Pour démontrer nos développements dans la direction de l'objectif **(i)** du projet, nous avons transféré les composants les plus performants des **cellules planes** prototypes aux cellules pilotes. Pour la première fois, nous avons rapporté le cycle électrochimique de cellules planes au sodium et chlorure de nickel à haute température avec une grande surface active de ~ 90 cm^2. Les meilleurs résultats ont été obtenus pour une charge cathodique de 80 mAh/cm^2, avec une capacité cumulée de 3,4 Ah/cm^2 obtenue pour un cyclage de plus de 2,5 mois à de faibles densités de courant (jusqu'à 10 mA/cm^2 pendant la charge, jusqu'à 20 mA/cm^2 pendant la décharge). Cependant, les variations géométriques et les tolérances dimensionnelles des composants de la cellule, en particulier des pièces en céramique frittée, empêchent un montage précis, une gestion efficace des matériaux fondus et une fermeture hermétique des cellules planes pilotes, ce qui compromet la durée de vie du cycle au stade actuel du

développement. En outre, nous avons identifié que les composants passifs nécessaires le long de la circonférence des cellules planes entraînent un poids et un coût supplémentaires dans cette géométrie. Ainsi, bien que les avantages d'une conception de cellules planes offrent certainement un potentiel pour une production à grande échelle, des matériaux de cellules alternatifs et/ou l'empilement de cellules dans une unité doivent être adoptés afin d'éviter une augmentation du poids des cellules. Au stade actuel, ces modifications doivent être étudiées plus avant pour répondre aux exigences de sécurité et de durée de vie des batteries commerciales à haute température.

Le nickel de la cathode contribuant de manière significative au coût et au poids des batteries au sodium et chlorure de nickel, nous avons poursuivi le développement de formulations de cathodes améliorées avec une **teneur réduite en nickel**. En introduisant un additif de carbone et en améliorant la préparation de la cathode, nous avons pu réduire la teneur en nickel jusqu'à 20 % en poids (-25 g par cellule), ce qui non seulement réduit le coût et le poids de la cathode, mais augmente également ses performances en termes de temps de charge, d'énergie de décharge et de durée de vie. Pour démontrer nos développements vers l'objectif **(ii)** du projet, nous avons intégré avec succès les formulations de cathode améliorées dans des cellules pilotes de nouvelle génération de géométrie tubulaire. La stabilité à long terme a été étudiée à l'aide de tests modulaires sur 10 cellules tubulaires de chaque composition, en appliquant une procédure de test de durée de vie allant jusqu'à 6 mois. Par rapport à l'état de l'art, les formulations améliorées maintiennent des temps de charge plus courts et des énergies de décharge plus élevées pendant le cyclage à long terme (par exemple, 10,5 h contre 12,0 h ; 386 contre 346 Wh/kg après 200 cycles de vie, 4 mois). Elles présentent également un taux de dégradation plus faible et devraient conserver 80 % de la puissance de décharge des cathodes standard après près de 7 000 cycles. Ainsi, alors que les réductions de coûts résultant de la réduction de la teneur en nickel sont modérées (par exemple -5 $/kWh, pour un prix du Ni255 de 20 €/kg), l'augmentation simultanée de la durée de vie peut réduire de manière significative les coûts énergétiques globaux résultants à 0,04-0,05 $/kWh/cycle. FZSoNick prévoit de mettre en œuvre les nouvelles formulations de cathodes à teneur réduite en nickel dans la production de ses batteries, à partir du début de 2023.

Nos développements sur les cellules au sodium et chlorure de nickel planes et tubulaires au cours des quatre dernières années démontrent les valeurs et les limites des deux géométries. Les cellules planes offrent une grande flexibilité, puisqu'elles peuvent intégrer des cathodes de différentes capacités et densités de remplissage, ainsi que des collecteurs de courant variables à l'anode et à la cathode. Le développement de cellules planes au sodium et chlorure de nickel à haute température dans le cadre du projet HiPerSoNick fait progresser de manière significative la recherche et le développement dans ce domaine. Cependant, les cellules tubulaires au sodium et chlorure de nickel les plus modernes offrent toujours une résistance de cellule plus faible et donc une énergie de décharge plus élevée que les cellules planes de laboratoire actuelles, pour une même charge cathodique. En outre, la fermeture hermétique de grandes cellules planes (>3 cm^2), permettant un cyclage stable à long terme à des températures de fonctionnement de ~300 °C dans l'air ambiant, n'a pas été démontrée jusqu'à présent. Des développements supplémentaires sont nécessaires pour améliorer leur conception, à la fois en termes de durée de vie en cyclage, de résistance de la cellule, de poids/volume de la cellule, de fiabilité et de rentabilité. Les cellules tubulaires imposent un certain nombre de contraintes, par exemple sur le volume et la densité de remplissage des granules cathodiques, mais offrent une faible résistance de la cellule et un cycle efficace à long terme.

Sur la base des compétences développées durant le projet HiPerSonick, tant en termes de développement de cellules planes que de modifications de la cathode, l'Empa et FZSoNick développent actuellement des formulations cathodiques alternatives dans le cadre du projet Horizon 2020 "Sodium-zinc molten-salt batteries for low-cost stationary storage (SOLSTICE)" (www.solstice-battery.eu), dans lequel le nickel est remplacé par du zinc moins coûteux.

Summary

The HiPerSoNick project focused on the development of next-generation cells for high-temperature sodium-nickel chloride batteries. Already a well-proven solution for backup power applications, this clean, efficient, and safe technology suffers from low charge rates and limited power density at high discharge currents. Commercial sodium-nickel chloride cells with tubular geometry contain a nominal capacity of 38-40 Ah at an active area of ~260 cm^2 (cathode loading ~150 mAh/cm^2). Operated at temperatures of around 300 °C, the cells are rated for continuous operation at high discharge current densities of 50 mA/cm^2. This translates into relatively low discharge rates of C/3, given the high cathode loading. Furthermore, production costs of the tubular high-temperature cells are relatively high, compared to lithium-ion batteries. Costs of high-temperature sodium-nickel chloride battery packs currently amount to 300–350 $/kWh, resulting in overall energy costs of 0.07–0.08 $/kWh/cycle, considering a design life of 4500 cycles. As shown in this project, state-of-the-art tubular cells can provide discharge energies of ~350 Wh/kg in long-term cycling studies at C/3 (relative to the cathode mass).

In the HiPerSoNick project, we conducted a comprehensive co-development of cell design, electrolyte, sealants, and electrodes. The two major project goals were **(i)** to demonstrate the feasibility of a **planar cell design**, and **(ii)** to **reduce the nickel content** of the cathode, in both cases without compromising performance and cycle life of the battery. Transfer from a tubular to a planar cell design shows potential to decrease production costs, as planar components are more compatible with automated high-volume manufacturing and quality control routines. The development of planar sodium-nickel chloride cells has been a focus of the research community for more than 10 years, but previous studies were restricted to small cells (e.g. 3 cm^2 active area), with a focus on moderate cathode loadings (50 mAh/cm^2) and low current densities (10 mA/cm^2). In this project, we first developed a versatile planar prototype cell platform with ~3 cm^2 active area. In symmetric cells, we demonstrated stripping and plating of molten sodium at extremely high current densities (up to 2600 mA/cm^2), without sodium metal dendrite formation. In full cells with moderate cathode loading (50 mAh/cm^2), we achieved the highest specific discharge energy reported in literature for extended cycling of planar high-temperature sodium-nickel chloride cells so far (277 Wh/kg for standard cathodes consisting of nickel complemented by iron, averaged over 50 cycles; discharge at 80 mA/cm^2, 1.6C). We further developed a number of passive cell components to manage the (partially) molten and corrosive materials in the cells also at high cathode loadings. For the first time, we achieved stable cycling of state-of-the art nickel/iron cathodes at a cathode loading of 150 mAh/cm^2, corresponding to what is employed in commercial tubular cells. At such high cathode loadings and discharge current densities of up to 80 mA/cm^2 (>C/2), we could demonstrate more than 50 stable cycles, while increasing the discharge energy even further (to >300 Wh/kg).

In a next step, we scaled the prototype cells to larger pilot cells (~90 cm^2 active area). To supply suitable planar ceramic electrolytes, we developed scalable shaping and sintering procedures for Na-β''-alumina. Our project provides two different successful procedures, based on either large-area tape casting and lamination or die pressing of Na-β''-alumina followed by sintering, resulting in robust planar Na-β''-alumina electrolyte disks with an area of ~95 cm^2. We further investigated temperature-resistant glass seals, which are critical for the long-term stability of planar cells, but also offer great potential for cost savings in tubular cells. We identified suitable glass seal candidates for the ceramic-to-ceramic and ceramic-to-metal joints required for cell assembly. In model experiments, we demonstrated the importance of the seal geometry and its processing, which provides a means to achieve the required low leak rates.

To demonstrate our developments towards project goal **(i)**, we transferred the most successful **planar cell** components from prototype to pilot cells. For the first time, we reported electrochemical cycling of planar high temperature sodium-nickel chloride cells at a large active area of ~ 90 cm^2. The best results

were obtained at a cathode loading of 80 mAh/cm^2, where a cumulative capacity of 3.4 Ah/cm^2 was cycled for over 2.5 months at low current densities (up to 10 mA/cm^2 during charge, up to 20 mA/cm^2 during discharge). However, geometrical variations and dimensional tolerances of the cell components, in particular of sintered ceramic parts, hinder precise fittings, efficient management of molten materials, and hermetic sealing of planar pilot cells, thus compromising the cycle life at the current stage of development. Furthermore, we identified the passive components required along the circumference of planar cells to result in additional weight and cost in this geometry. Thus, while the advantages of a planar cell design certainly offer potential for large-scale production, alternative cell materials and/or the stacking of cells in one unit need to be adopted in order to avoid an increase in cell weight. At the current stage, such modifications need further study to fulfil the safety and lifetime requirements of commercial high-temperature batteries.

Because the nickel in the cathode contributes significantly to cost and weight of sodium-nickel chloride cells, we further developed enhanced cathode formulations with **reduced nickel content**. By introducing a carbon additive and improving the processing, we could reduce the nickel content by up to 20 wt% (-25 g per cell), which not only reduces the cost and weight of the cathode, but also increases its performance in terms of charge time, discharge energy, and cycle life. To demonstrate our developments towards project goal **(ii)**, we successfully integrated the enhanced cathode formulations in next-generation pilot cells of tubular geometry. The long-term stability was investigated by module tests on 10 tubular cells of each composition, applying a life-test procedure for up to 6 months. Compared to state-of-the-art cathodes, the enhanced formulations maintain lower charge times and higher discharge energies during long-term cycling (e.g. 10.5 h vs. 12.0 h; 386 vs. 346 Wh/kg after 200 life cycles, 4 months). They also provide a lower degradation rate, and are projected to maintain 80% of the discharge power of standard cathodes after almost 7000 cycles. Thus, while cost reductions from reducing the nickel content are moderate (e.g. -5 $/kWh, at a Ni255 price of 20 €/kg), the concurrent increase in cycle life can significantly reduce the resulting overall energy costs to 0.04–0.05 $/kWh/cycle. FZSoNick is planning to implement the newly developed cathode formulations with reduced nickel content in the production of their batteries, starting at the beginning of 2023.

Our developments on both planar and tubular sodium-nickel chloride cells over the past four years demonstrate the values and limitations of both geometries. Planar cells offer great flexibility, being able to integrate cathodes of different capacity and packing density, as well as variable current collectors at anode and cathode. The development of planar high-temperature sodium-nickel chloride cells in the HiPerSoNick project significantly advances research and development on this topic. However, state-of-the-art tubular sodium-nickel chloride cells still provide a lower cell resistance and thus higher discharge energy than present, laboratory-scale planar cells at the same cathode loading. Furthermore, hermetic sealing of large planar cells (>3 cm^2) enabling stable long-term cycling at operating temperatures of ~300 °C in ambient air has not been demonstrated so far. Further development is required to improve their design, both in terms of cycle life, cell resistance, cell weight/volume, reliability, and cost effectiveness. Tubular cells set a number of constraints, e.g. on volume and packing density of cathode granules, but provide low cell resistance and efficient long-term cycling.

Based on the competences developed during the HiPerSonick project, both in terms of planar cell development and cathode modifications, Empa and FZSoNick are currently developing alternative cathode formulations in the Horizon 2020 follow-up project "Sodium-zinc molten-salt batteries for low-cost stationary storage (SOLSTICE)" (www.solstice-battery.eu), in which nickel is replaced with lower-cost zinc.

Main findings

We developed two potent and versatile planar high-temperature cell platforms (prototype cells with 3 cm^2, and pilot cells with 90 cm^2 active area), which exceed the state-of-the-art for planar sodium-nickel chloride cells in several aspects:

- active cell area of planar sodium-nickel chloride cells, up to 90 cm^2
- cathode loading, up to 150 mAh/cm^2
- discharge current density and specific energy, up to 80 mA/cm^2, ≥300 Wh/kg (with respect to the cathode mass).

For the first time, we demonstrated scalable and reproducible processing routines for manufacturing of planar ceramic Na-beta''-alumina electrolyte disks (up to 95 cm^2).

While the advantages of a planar cell design may offer potential for large-scale production of cell stacks in the future, this technology is currently not mature enough for implementation into an industrial production.

Nevertheless, several components developed in this project, in particular the enhanced cathode formulations, show great potential for immediate implementation into the industrial production of next-generation sodium-nickel chloride (or more generally sodium-metal chloride) cells at FZSoNick, thereby strengthening this Swiss made battery type.

Contents

Abbreviations

C rate	charge/ discharge rate, current through battery relative to rated capacity
cathode loading	in mAh/cm^2, corresponds to the area-specific cell capacity, as cells are assembled in the absence of a sodium anode
ceramic subassembly	ceramic Na-β''-alumina electrolyte, sealed to insulating α-alumina collar
CV	cyclic voltammetry
CTE	coefficient of thermal expansion
(de-)chlorination	(reversible) chlorination and de-chlorination reaction
DOD	depth of discharge
DST	dynamic stress test
EDS	energy-dispersive x-ray spectroscopy
Na-β''-alumina	sodium-ion conducting ceramic electrolyte applied in Na-$NiCl_2$ batteries
Na-$NiCl_2$ battery	sodium-nickel chloride battery
Na-S battery	sodium-sulfur battery
OCV	open circuit voltage
SEM	scanning electron microscopy
SOC	state of charge
$NaAlCl_4$	sodium tetrachloroaluminate, molten salt applied as secondary liquid electrolyte at the cathode of Na-$NiCl_2$ cells
TCB	thermo-compression bonding
TOC	top of charge
WP	work package

1 Introduction

1.1 Background information and current situation

The development of high-temperature sodium batteries dates back to 1967, when researchers at Ford Motor Company first presented a rechargeable sodium-sulfur (Na-S) battery cell [1]. Towards a battery technology for motive power applications, they selected electrode materials in the molten state, providing a high mobility of electroactive species. A Na-β"-alumina ceramic as solid electrolyte provided an unprecedented match of high and selective ion conductivity with good mechanical and (electro-) chemical stability [2]. However, the highly corrosive molten sulfur cathode and its violently exothermic reaction in contact with sodium upon cell rupture impeded commercial applications of sodium-sulfur batteries, and triggered efforts to implement alternative cathode materials. This motivated research in a safer high-temperature technology, leading to a first patent application on high-temperature sodium-metal chloride (Na-$NiCl_2$) cells by CSIR in 1978 [3]. The new technology, which would later become the Na-$NiCl_2$ battery, took over the tried and tested Na-β"-alumina electrolyte and molten sodium anode from the sodium-sulfur technology. At the cathode, it applied solid transition metal chlorides, which were immersed in a molten salt electrolyte ($NaAlCl_4$) to enable fast reaction kinetics and a high mobility of electroactive species. After another decade, in 1998, AEG Anglo Batteries produced maintenance-free Na-$NiCl_2$ battery systems for electric vehicles in a pilot line, which offered higher energy density than the lead acid and NiMH batteries available at that time [4]. Soon after, an improved Na-$NiCl_2$ battery type was demonstrated, providing a specific energy >140 Wh/kg on cell level [5]. In 1999, the company MES-DEA acquired and industrialized the Na-$NiCl_2$ battery technology in Stabio, Switzerland [6], with a focus on electromotive applications. In a first phase, a production capacity of 40 MWh per year was implemented with a specific energy and power of 120 Wh/kg and 180 W/kg, with respect to the entire battery system [6,7]. In 2010, MES-DEA was bought by the Italian FIAMM group, which established the subsidiary FZSoNick. Until today, FZSoNick manufactures commercial Na-$NiCl_2$ batteries in Switzerland. The complete production line is covered locally, including (i) production, shaping and sintering of the ceramic electrolyte from raw materials, (ii) production of the cathode materials, (iii) cell assembly and testing, (iv) battery assembly and testing, (v) system design, (vi) system integration, including battery management system [6,7]. Their batteries are mainly deployed as back-up power source for telecom antennas, but show strong potential for large-scale grid storage needed for the implementation for renewable energy production [8–10]. Application of Na-$NiCl_2$ batteries has also been demonstrated for electric vehicles [11,12], residential prosumers [13], as part of a smart microgrid [14], and under peak-shaving duty cycles [15]. In 2011, General Electric (GE) entered development and fabrication of commercial Na-$NiCl_2$ batteries in the US under the tradename Durathon, with large-scale grid storage as a target market. However, the energy storage market failed to meet the investor's expectations, and GE ceased production of this battery technology in 2015 [16,17]. In 2017, a cooperation between GE and the Chilwee Group transferred the technology to China, where commercialization was announced in 2020 [18]. Also in Germany, the company Alumina Battery Systems announced commercialization of Na-$NiCl_2$ batteries for 2022 [19].

High-temperature Na-$NiCl_2$ batteries, operated at 250-340 °C, are an alternative to lithium-ion (Li-ion) batteries for stationary storage applications. This battery type avoids the use of critical and rare elements[20–22]. Using a liquid sodium metal anode, a solid-state ceramic sodium-β"-alumina electrolyte, as well as rock salt, nickel and iron as active cathodes materials[23], it is constituted exclusively of abundant raw materials. Due to their lower self-discharge rate compared to lithium-ion batteries, sodium-nickel-chloride batteries qualify for backup power applications in mobile telecommunication antennas[9,24], but also show great potential for large-scale stationary electricity storage[8,10]. At the current stage of development, sodium-nickel-chloride batteries provide gravimetric energy and power

densities of 140 Wh/kg and 180 W/kg on cell level, at a nominal cell voltage of 2.5 V [8,12]. Their cell design is similar to high-temperature sodium-sulfur (Na-S) batteries, which employ the same materials as solid electrolyte (sodium-β"-alumina) and anode (molten sodium), but a sulfur-based cathode[25]. Sodium-sulfur batteries provide a lower nominal cell voltage (2.1 V), as well as lower energy and power densities (typically 120 Wh/kg and 100 W/kg on cell level[26]). While energy and power density of both types of high-temperature sodium batteries are significantly lower than for Li-ion batteries on cell level (see **Table 1**), this comparison turns more favorable when considering the whole battery system. Due to the narrow optimal operating temperature of 15-35 °C for lithium-ion batteries, additional weight for both heating and cooling functionality is required for large-scale Li-ion batteries[27]. In contrast, sodium-nickel-chloride batteries require heating only. And while up to 10% capacity loss per day may be necessary to compensate heat losses in idle high-temperature batteries[6], large Na-$NiCl_2$ batteries can maintain their operating temperature by ohmic cell heating under favorable load profiles[28]. Thus, the main performance challenge for high-temperature batteries to compete with Li-ion batteries for stationary applications is their lower specific power. Furthermore, the overall cost of energy storage critical for large-scale applications. Low system costs of 100 – 200 $/kWh have been projected for sodium-nickel-chloride batteries[28,29], which results in competitive overall energy costs of <0.02 – 0.04 $/kWh/cycle, considering a design life of 4500 cycles[30]. However, these projections do not take into account the costs for assembly and components of high-temperature battery cells. As a result, current production costs do not yet allow to reach these values. Costs of high-temperature sodium-nickel chloride battery packs currently amount to 300–350 $/kWh, resulting in overall energy costs of 0.07 – 0.08 $/kWh/cycle, considering a design life of 4500 cycles[30]. Commercial Na-$NiCl_2$ cells with tubular geometry contain a nominal capacity of 38-40 Ah at an active area of ~260 cm^2, corresponding to a high cathode loading of ~150 mAh/cm^2. Applying a cost-efficient, mixed nickel and iron cathode, they are rated for discharge at C/3, 50 mA/cm^2. Based on long-term cycling experiments performed on tubular cells in this study, such tubular cells with mixed Ni/Fe cathode deliver discharge energies of ~350 Wh/kg, relative to the cathode mass (see report below). Despite the high current densities applied, commercial ZEBRA batteries provide high cycle efficiencies of 90%. This is enabled by a low cell resistance, which takes values of ~4 Ωcm^2 (15 mΩ, 260 cm^2 active area)[31]. The influence of cell resistance on energy efficiency can be estimated by a simple calculation: Assuming charge and discharge at typical current densities of 20 mA/cm^2 and 50 mA/cm^2 for nickel de-/chlorination at 2.58 V, a cell resistance of 4 Ωcm^2 indeed translates to an energy efficiency of ~90% per cycle. Doubling or tripling the cell resistance (to 8 Ωcm^2, 12 Ωcm^2) at the same conditions reduces the cycle efficiency to 80% and 70%, respectively.

Recent scientific literature focuses on developing Na-$NiCl_2$ batteries with planar cell geometry, for which processing can be scaled more efficiently[32]. This is often combined with operation at reduced temperatures of ~200 °C, where the use of polymer seals facilitates cell assembly[33]. The highest discharge energy reported for planar Na-$NiCl_2$ cells so far amounts to 350 Wh/kg, relative to the cathode mass[34]. This was demonstrated for laboratory-scale cells with moderate cathode loading at 190°C (3 cm^2 active area, 50 mAh/cm^2), which delivered impressive long-term stability over 1000 cycles, but low discharge power density (75 W/kg, relative to cathode mass)[34]. The planar cells with Fe-free Na-$NiCl_2$ cathode further showed a large voltage hysteresis between charge and discharge (>200 mV), despite the low charge current (7 mA/cm^2) and discharge power (75 mW/cm^2, ~10 mA/cm^2) applied[34]. This indicates a high cell resistance (>10 Ω cm^2), which would significantly reduce the energy efficiency when scaled to commercially relevant cathode loading and charge/discharge rates. Increasing the operating temperature can significantly reduce the cell resistance, especially at high areal capacity. However, the highest discharge energy previously reported for planar, laboratory-scale Na-$NiCl_2$ cells at 280 °C amounts to only 160 Wh/kg (demonstrated over 60 cycles) [35,36].

Another important field of development is the cathode composition of Na-$NiCl_2$ batteries. To maintain electronic conductivity in the electrode during cycling at all states of charge, nickel is applied in excess

quantities. Typically, the active metal content used for electrochemical cycling is only about 30% [5]. Together with the presence of additives, this reduces the gravimetric capacity of state-of-the-art nickel and iron chloride electrodes from >300 mAh/g to 160 mAh/g.

Table 1 Comparison of Li-ion, NaS, and Na-$NiCl_2$ batteries, data from [12,26,37–39].

	Li-ion	NaS	NaNiCl
Energy density, cell level [Wh/kg]	250	120	140
Power density, cell level [W/kg]	500	100	180
Nominal cell voltage [V]	3.7	2.1	2.5
Ideal operating temperature [°C]	15-35	350	300

1.2 Purpose of the project

Major advantages of Na-$NiCl_2$ batteries in the current market situation are their long lifetime, safe and emission-free operation, large operation temperature window, and the abundance of raw materials required for production. However, the battery market in general is currently strongly dominated by the Li-ion technology, offered at aggressive pricing. Na-$NiCl_2$ batteries provide benefits for stationary applications, but the technology faces challenges in terms of production cost. It is therefore necessary to perform a re-assessment of the Na-$NiCl_2$ technology in terms of cell design, materials development, and processing routines in order to strengthen its competitiveness.

In this context, one goal of the HiPerSoNick project is to (i) assess the potential of a planar high-temperature Na-$NiCl_2$ cell design for commercial applications. A second goal is to (ii) enhance the performance and cost-efficiency of tubular high-temperature Na-$NiCl_2$ cells, in particular by a reduction of nickel content at the cathode, corresponding to an increase in active metal content.

1.3 Objectives

The HiPerSoNick project wants to provide a comprehensive co-development of cell design, electrolyte, and electrode systems to boost the cost-efficiency and cycle life of Na-$NiCl_2$ batteries. The specifications of state-of-the-art tubular Na-$NiCl_2$ cells, as well as the project targets, are summarized in **Table 2**. Due to the significant cost contribution of cell assembly and passive components, a similar (or higher) cell capacity as in state-of-the-art tubular Na-$NiCl_2$ cells is considered necessary for next-generation cells (150 mAh/cm^2). An increase in nominal energy density on cell level can be achieved by increasing the specific cathode capacity, by increasing the ratio of capacity to mass of nickel (increasing the active nickel content), and/or by decreasing the cell weight. An increase in nominal discharge rate, and a decrease in charge duration for 10-100% SOC, could enable the use of Na-$NiCl_2$ batteries in a broader field of applications, thereby increasing its market share. Finally yet importantly, an increase of service life directly reduces the cost of overall energy costs per cycle.

Table 2 Specifications for state-of-the-art tubular Na-$NiCl_2$ cells, and targets for the HiPerSonick project.

	state-of-the art tubular cell	project targets
cell capacity	40 Ah, 150 mAh/cm^2	150 mAh/cm^2
nominal energy density on cell level*	140 Wh/kg	160 Wh/kg
↳ specific cathode capacity	160 mAh/g	180 mAh/g
↳ ratio of capacity to mass of Ni	0.3 Ah/g	0.4 Ah/g
↳ and/or cell weight	700 g	620 g
nominal discharge rate	C/3, 50 mA/cm^2	C/2, 75 mA/cm^2
max. discharge rate (30 s pulse)	1.5C, 225 mA/cm^2	1.5C, 225 mA/cm^2
charge duration, 10-90% SOC	5 h	5 h
charge duration, 10-100% SOC	10 h	8 h
projected service life	4500 cycles	7000 cycles

*The nominal energy density on cell level is defined as the product of cell capacity, cell weight, and a nominal discharge voltage of 2.5 V.

2 Procedures and methodology

Na-$NiCl_2$ batteries operate at high temperatures of ~300°C. Their anode and cathode compartments require separate hermetic seals to avoid mass transfer, both between each other, and with the outside environment. Furthermore, the molten phases (sodium at the anode, $NaAlCl_4$ as secondary electrolyte at the cathode) need to be confined, while balancing the volume changes of all components with variable temperature and, in particular, with variable state-of-charge. The development of a suitable characterization environment was therefore of paramount importance for the assessment of all cell components.

In **WP1** of this project, we first developed planar Na-$NiCl_2$ prototype cells of 3 cm^2 active area (**Figure 1a,d,e**), which allow electrochemical characterization of electrodes with relevant areal capacity (150 mAh/cm^2). The focus for the development of the prototype cells was to provide high flexibility to characterize variable passive and active cell components. The planar cells further served to analyze the complex electrochemical processes in state-of-the-art and enhanced Na-$NiCl_2$ cathodes, thus identifying critical or rate-limiting processes and components.

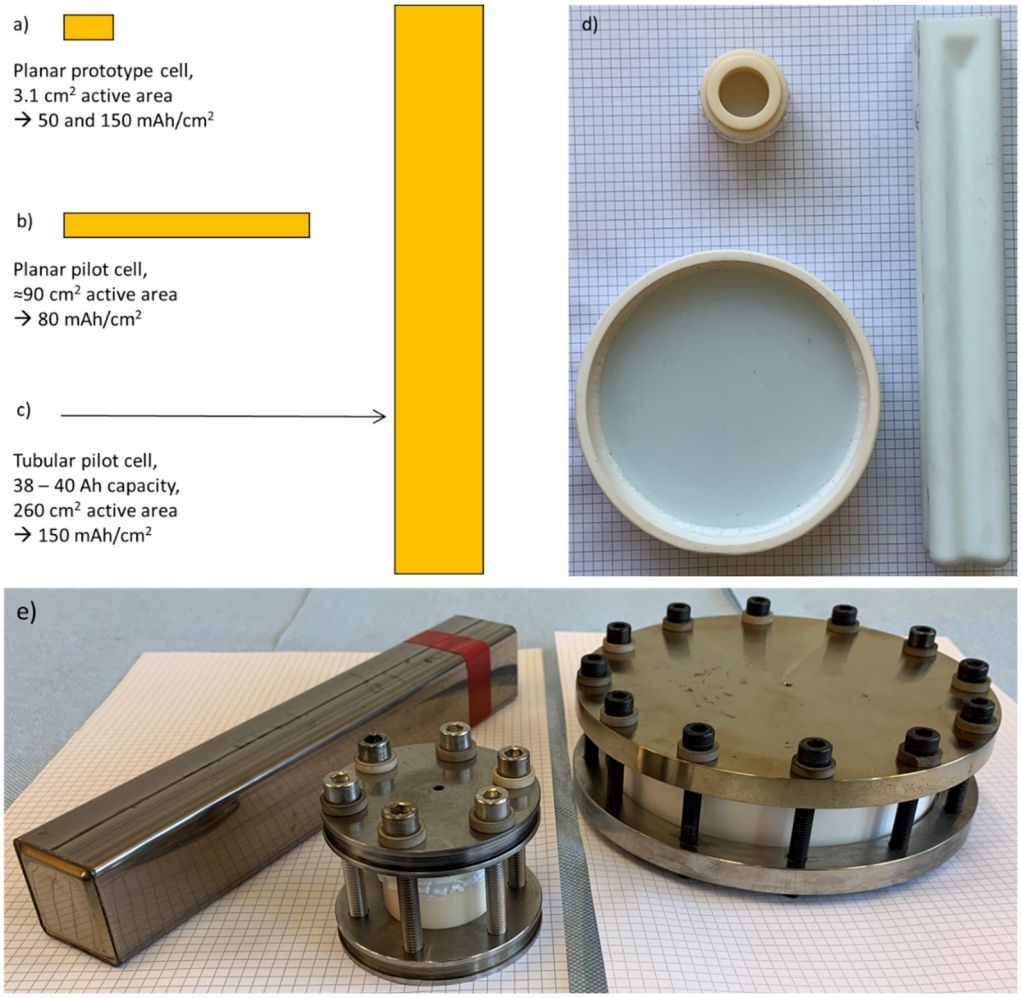

Figure 1 Different high-temperature cells developed in the HiPerSoNick project. Dimensions of **a)** planar prototype cell (WP1), **b)** planar pilot cell (WP1, WP5), **c)** tubular pilot cell (WP4, WP5). Photographs of **d)** ceramic subassemblies and **e)** battery cells of prototype, planar pilot, and tubular pilot.

The development of robust Na-β''-alumina electrolytes with large area is a prerequisite for the Na-$NiCl_2$ technology (**WP2**). State-of-the-art Na-$NiCl_2$ cells are based on tubular electrolytes with cloverleaf-shaped cross section, featuring an active area of 260 cm^2. In this project, we enhanced the processing of Na-β''-alumina and developed scalable processing routines for planar Na-β''-alumina electrolytes with a diameter >10 cm (~95 cm^2) by tape casting, lamination, and sintering (**Figure 1d**). We further applied uniaxial pressing and sintering to prepare planar electrolytes of the same size.

Safe operation and long-lifetime of Na-$NiCl_2$ batteries are only possible with robust hermetic seals (**WP3**). Two types of functional seals are required: (1) between the sodium-ion conducting ceramic β''-alumina and the ceramic α-alumina insulator, and (2) between the α-alumina insulator and the metallic current collectors. In both cases, the seals need to withstand exposure to the molten electrode materials. Increasing active area and seal lengths in planar geometries is a major obstacle in the development of planar high-temperature devices. While excellent seals (low helium leak rate <10^{-7} mbar L/s, long lifetime >25 years) are available for state-of-the-art tubular cells, their processing at 1010 °C sets severe constraints for the assembly of cells. Exploration of alternative low-temperature sealants was thus another important aspect of this project, both for tubular and planar cell geometries.

In the course of the project, the design and assembly of planar prototype and pilot cells was developed as follows.

Ceramic subassembly:

Planar prototype cells are assembled from two α-alumina collars (99.7% Al_2O_3, inner diameter 20 mm) and one Na-β"-alumina solid electrolyte disc. Na-β"-alumina discs are prepared by pressing spray-dried Li-stabilized Na-β"-alumina powder (FZSoNick) into disc-shaped green bodies with a diameter of 45 mm and a thickness of approximately 4 mm. The green bodies are placed onto buffer green discs, and sintered inside a ceramic encapsulation in static air at 1600 °C. Subsequently, the sintered Na-β"-alumina discs are ground down to a thickness of 1 mm, and then glass sealed between the two α-alumina collars using a high-temperature glass sealing at 1010 °C (FZSoNick) to obtain a ceramic subassembly. **Planar pilot cells** are assembled from one L-shaped α-alumina collar and one Na-β"-alumina solid electrolyte disc. Large Na-β"-alumina solid electrolyte discs with ~110 mm diameter are produced by either tape-casting or pressing.

Electrode materials:

Both planar prototype and pilot cells use FZSoNick's state-of-the art millimeter-sized cathode granules and secondary electrolyte $NaAlCl_4$. The granules contain: Ni (50 wt.%, filamentary Ni255), Fe (7 wt.%), Al (0.5 wt.%), micro-fine NaCl (39 wt.%), and the following additives: FeS (2 wt.%), NaF (2 wt.%), and NaI (0.5 wt.%). Both planar prototype and pilot cells focus on a loading of cathode granules of 150 mAh/cm^2, with additional experiments at 50 mAh/cm^2. Molten $NaAlCl_4$ is vacuum infiltrated into the granules at a pressure of less than 10 mbar and a temperature of 200 °C (dwell time ~20 min). A small portion of Na is added into the anode compartment of both cell types to facilitate the maiden charge.

Cell assembly and cycling of planar cells:

Both planar prototype and pilot cells are assembled and cycled in an Ar-filled glovebox. The planar cells are compressed between stainless steel top and bottom plates using stainless steel bolts and alumina washers for electrical insulation. Graphite or metal seals are placed between the α-alumina collars and the top and bottom plates to seal the cell towards the outside. Inside the cell, Ni-wires fixed by screws connect the backside of the Ni pistons with the stainless steel top and bottom plates, to bypass the electrical resistance of the springs.

Electrode composition, microstructure and processing define the heart of the Na-$NiCl_2$ technology. In **WP4**, we modified the cathode composition in order to reduce its nickel content. However, detection and analysis of changes to the cathode material on long-term battery performance is difficult, requiring highly reproducible cell production to obtain reliable electrochemical data. Such data is accessible from cycling experiments in state-of-the-art tubular Na-$NiCl_2$ cells (**Figure 1c,d,e**), which we applied to characterize new cathode compositions in this project. Tubular cells provide tight seals, high cathode loading (~150 mAh/cm^2), large active area (~260 cm^2), and optimized cell components, resulting in excellent capacity retention, low internal cell resistances (≈ 10 mΩ), and reproducible cycling behavior.

In a first experimental series, we prepared Na-$NiCl_2$ cathodes with reduced nickel content, and evaluated their performance in tubular cell modules by a dynamic stress test procedure at FZSoNick (DST, USABC Procedure #5B, 1994; in ambient atmosphere). Cell modules, comprising 10 tubular cells, were first subjected to a run-in procedure to stabilize their cycling performance (10 charge-discharge cycles, ~2 weeks). Then, a reference discharge was recorded (at 31 mA/cm^2, lower cut-off voltage 2.05 V). The conditions for the DST procedure were scaled to the Na-$NiCl_2$ cells according to the specifications summarized in **Figure 2a**. Examples of a resulting DST microcycle, of a number of microcycles required to perform discharge to 10% depth of discharge (DOD), and of 50 DST block are shown exemplarily in **Figure 2b-d.** 50 DST blocks correspond to continuous cycling over ~1 month.

a) Conditions for DST procedure

nominal capacity	38 Ah
peak discharge power	190 W/kg on cell level → **130 W** (100 % of peak pulse power)
discharge to 10 % DOD	**34.2 Ah**
charge procedure	const. current (5 A) to 2,67 V (cell) const. voltage (2,67 V) to I ≤ 0,15 A
voltage limitation	1.72 V – 2.85 V
operating temperature	270 °C

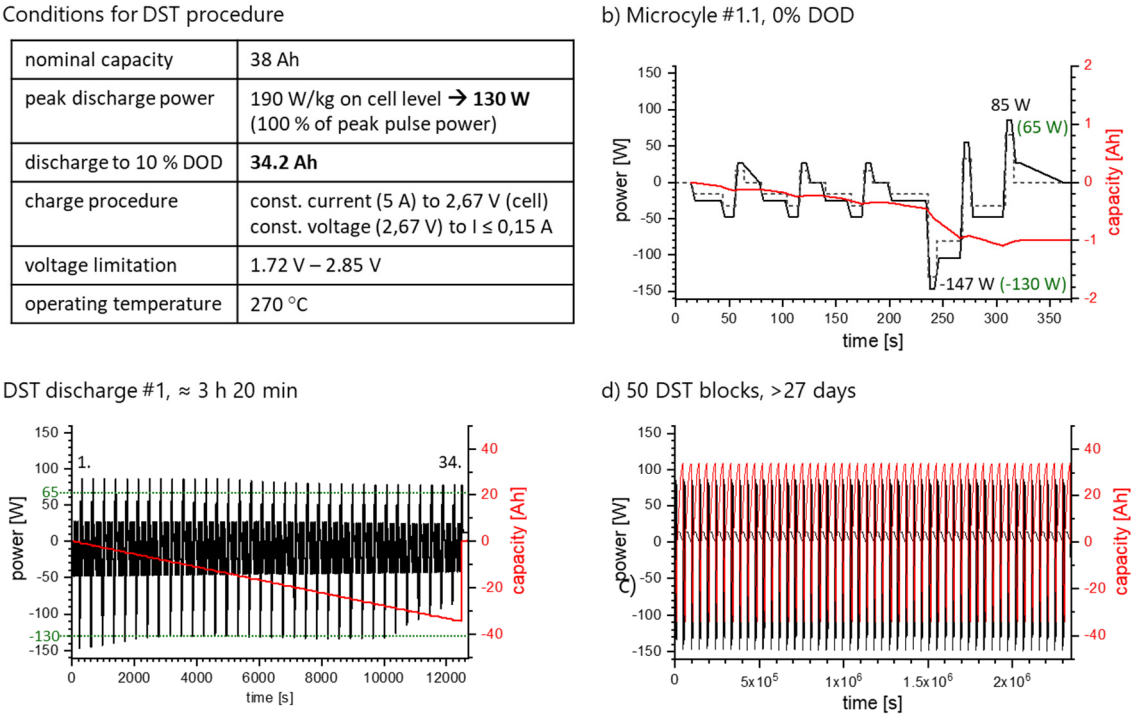

Figure 2 Dynamic stress test (DST) procedure applied to characterize Na-$NiCl_2$ cells in WP4 (at 270 °C). **a)** Conditions applied to scale the DST procedure to Na-$NiCl_2$ battery cell specifications. **b)** DST microcycle, **c)** DST discharge cycle, comprising 34 microcycles, and **d)** 50 DST blocks, comprising 50 DST charge and discharge cycles, shown exemplarily for a cell module with ~4g Ni.

For the final phase of the project (**WP5**), both planar and tubular next-generation Na-$NiCl_2$ pilot cells were prepared. Thermal and mechanical assessments were combined with electrochemical modeling to assist the design of improved active and passive components for planar pilot cells. Planar pilot cells with standard Ni/Fe cathode (**Figure 1b,d,e**, ~90 cm^2 active area, cathode loading ~80 mAh/cm^2) were prepared and characterized at Empa in a glovebox environment. Cycling was performed at constant currents between 2 and 20 mA/cm^2, followed by constant voltage charge and discharge at upper and lower cut-off potentials of 2.72 V and 1.8 V.

Tubular pilot cells (**Figure 1c**, ~260 cm^2 active area, cathode loading ~150 mAh/cm^2) were characterized in regular module tests at FZSoNick (strings of 10 tubular cells, testing in ambient atmosphere). This procedure was developed at FZSoNick to analyze the aging of Na-$NiCl_2$ batteries. To stabilize the cell performance, all modules were first subjected to a run-in procedure (~20 cycles). Then, the life-test procedure was applied at 270 °C in blocks of 50 cycles (test duration of ~1 month). Each life test cycle combines continuous discharge over 38 Ah at C/3 (13 A, 50 mA/cm^2) with two current pulses of 60 A (231 mA/cm^2) and 30 A (150 mA/cm^2, **Figure 3**). Between the blocks, additional characterization cycles were performed (14 cycles, constant-power discharges, 40-80-100-120 W, at 270 °C and 245 °C, followed by constant-current discharges, 4-8-20-40-60-80 A, at 270 °C).

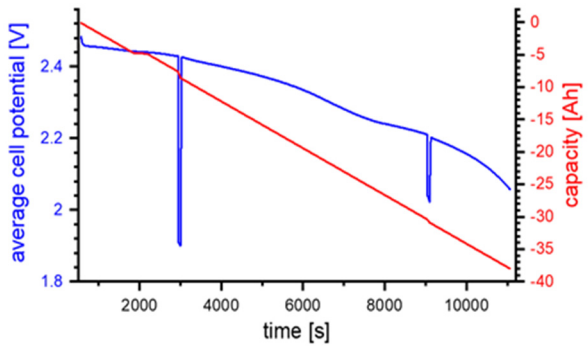

Figure 3 Discharge cycle of the life test procedure applied to characterize Na-$NiCl_2$ cells in WP5 (~3h, at 270 °C). Discharge at C/3 (13 A, 50 mA/cm^2) over 38 Ah, with a current pulses of 60 A (1.5C, 230 mA/cm^2) over 60 s at 20% DOD, and a current pulses of 30 A (1C, 150 mA/cm^2) over 60 s at 80% DOD. Charge was performed at a constant rate of C/8 (5 A, 19 mA/cm^2) to a cell potential of 2.67 V, followed by constant voltage charging (charge time ~12 h).

3 Results and discussion

3.1 WP1: Planar prototype cells

One of the main challenges in the development of Na-$NiCl_2$ cells is to contain and manage the active materials in hermetically sealed electrode compartments at elevated operating temperatures of ~300 °C. The electrode materials contain molten and highly reactive phases (sodium at the anode, and $NaAlCl_4$ at the cathode) and are subject to significant volume changes, both due to thermal expansion, and due to the electrochemical reactions of the active materials at different state-of-charge. Nevertheless, electronic contact and all necessary mass transport paths through the electrochemical cell need to be assured at all times. In commercial Na-$NiCl_2$ cells, sophisticated engineering and production processes provide both an efficient management of molten phases, and protection from unintended side reactions, enabling a battery design life of 20 years and >4500 cycles.
In the HiPerSoNick project, we designed, constructed, tested, and repeatedly debugged planar high-temperature prototype cells of 3.1 cm^2 active area, which can now operate successfully at temperatures up to 350 °C **(Figure 4**). Details on the cell development are summarized in a PhD thesis performed within the project ([Landmann2022PhD], chapter 2). Prototype cells are assembled and cycled in an Ar-filled glovebox. In the course of the project, six independent cycling units for high-temperature prototype cells were set up at Empa.

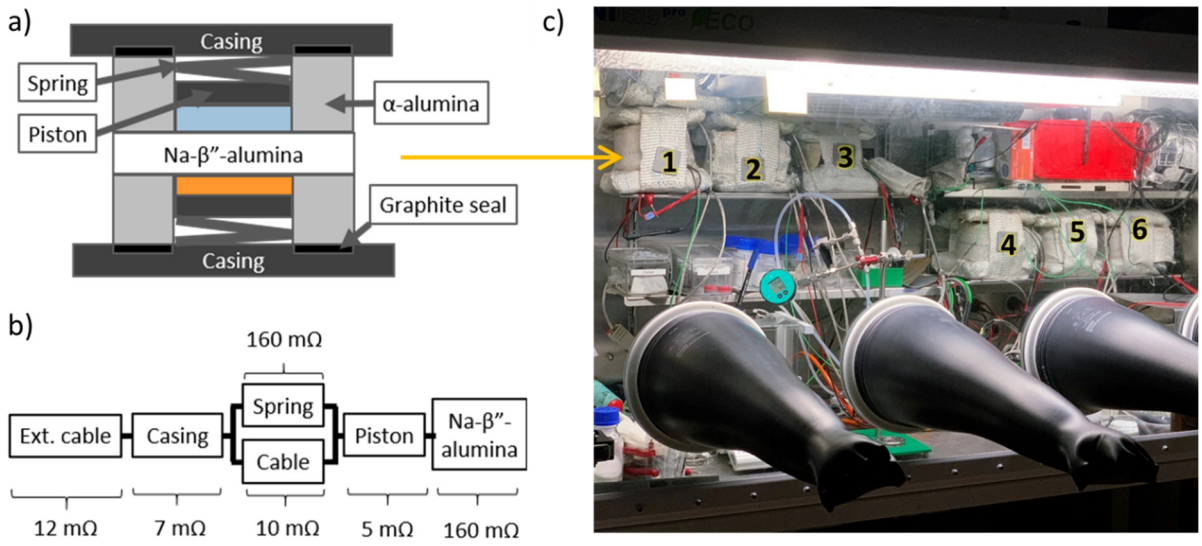

Figure 4 a) Drawing of **planar prototype cell design** for operation temperatures up to 350 °C. b) Equivalent circuit for one half of the cell, including external connection cables and Na-β"-alumina at 300 °C (1mm thick, 20 mm diameter). Source: [Landmann2022PhD]. c) Characterization of up to six prototype cell assemblies in a glovebox at Empa.

To validate the functionality of the prototype cell, we first studied the electrochemical performance of **symmetrical Na/Na-β"-alumina/Na cells** at different temperatures and current densities *[Landmann2020]*. To prevent dewetting of liquid sodium from the Na-β"-alumina electrolyte surface, we applied a porous carbon coating (similar to commercial tubular cells). For room temperature batteries, reversible plating and stripping of alkali metal anodes over many cycles without alkali metal dendrite formation is a severe challenge. This is related to voids forming in solid alkali metal anodes at the interface to the solid electrolyte upon stripping, which leads to mass-transport limitations. In contrast, above the melting temperature of sodium (140 °C, 250 °C), we could cycle the symmetrical prototype cells at extremely high current densities up to 2600 mA/cm^2 without dendrite formation (**Figure 5**). For comparison, the current density targeted by the US Department of Energy for fast-charging battery applications amounts to only 10 mA/cm^2 [40]. This shows that electrolyte, active and passive cell components, and interfaces of our planar high-temperature cells are very stable under relevant electrochemical cycling conditions. Furthermore, our experiments reveal that the negative electrode does not limit the overall rate-performance of sodium-nickel-chloride batteries, which is therefore dominated by the positive electrode. Last but not least, we developed an open cell design, which provides visual access to the top electrode of Na/Na-β"-alumina/Na cells. For the first time, this visualizes the movements of molten sodium in high-temperature planar cells upon cycling.

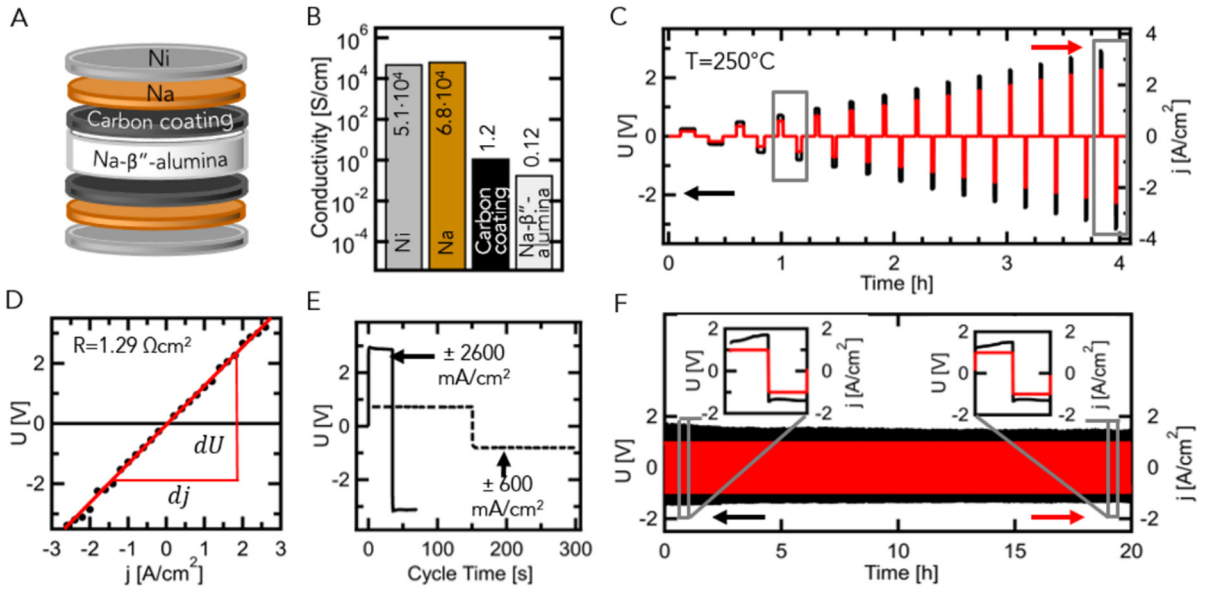

Figure 5 **Symmetrical prototype cell** at 250 °C. a) Schematic of the symmetric cell: Na/Na-β"-alumina/Na, with 250 µm thick carbon coating. b) Electronic conductivity of nickel, liquid sodium, and carbon coatings, compared to the ionic conductivity of Na-β"-alumina at 250 °C. c) Plating/stripping cycles with stepwise increase (200 mA/cm^2) of applied current density j (red line) up to 2600 mA/cm^2, and corresponding voltage U response of the cell (black line). d) Corresponding cell voltage U as a function of current density j, showing a linear relationship and constant cell resistance of 1.29 Ωcm^2. e) Magnified view of plating/ stripping cycles at 2600 and 600 mA/cm^2, respectively. f) Cumulative plating of 10 Ah/cm^2 at 1000 mA/cm^2 (400 cycles). Source: [Landmann2020].

The planar prototype cell platform further enabled us to study the mechanisms of **nickel and iron** chlorination during cycling of **disc-shaped model electrodes** [Landmann2022]. Our results demonstrate that metal-ion diffusion and metal-ion solubility in the molten $NaAlCl_4$ electrolyte limit the rate capability of planar nickel and iron cathodes, rather than transport across the metal chloride layer as previously suggested in literature (**Figure 6**). Thus, the presence of soluble cathode species does not necessarily decrease the reversibility of the redox reactions in sodium-metal chloride batteries. These mechanistic understandings open the field for a rational design of alternative cathode compositions also beyond this project. In particular, they are important for zinc-based batteries, which could provide a cost-efficient alternative to the nickel-based batteries. This is a basis for the follow-up project on "Sodium-zinc molten-salt batteries for low-cost stationary storage (SOLSTICE)", which was granted by the EU Horizon 2020 funding program to a consortium of 11 European partners, including Empa and FZSoNick (7.7 M€ from 2021-2024).

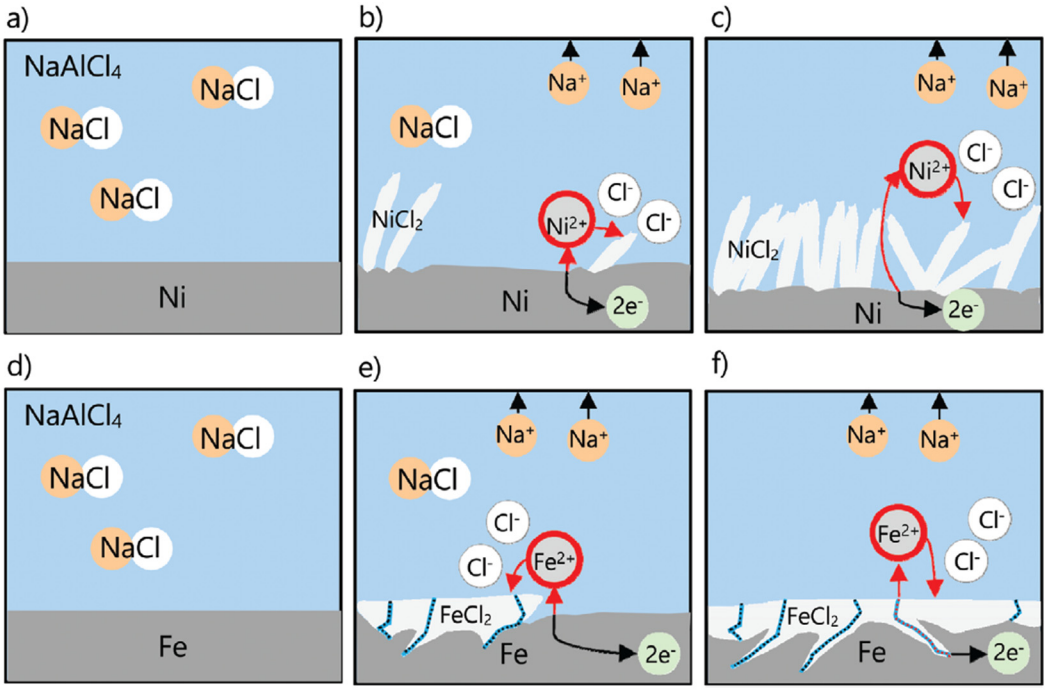

Figure 6 Sketch comparing chlorination mechanism of a-c) nickel and d-f) iron surfaces at 0, 0.015, and 0.5 mAh/cm^2 state-of-charge in prototype cells with **disc-shaped model electrodes**. Source: [Landmann2022].

In a next step, we employed the planar high-temperature **prototypes** in battery **full cells** at 300 °C [Graeber2021]. At the positive electrode, we integrated cathode granules prepared by FZSoNick. To immerse the cathode granules in the molten salt electrolyte ($NaAlCl_4$), we developed a vacuum-infiltration procedure. For comparison with available literature, we first applied a **moderate cathode loading of ≈50 mAh/cm²** (1/3 of state-of-the-art tubular cells). Our cells show an excellent cycling performance, both for state-of-the art Fe/Ni cathodes (**Figure 7a**), but in particular for iron-free nickel cathodes (**Figure 7b**). For state-of-the-art Fe/Ni cathodes, we could demonstrate stable cycling at 80 mA/cm² (1.6C) between 10% and 90% SOC for more than 50 cycles (+ run-in procedure, cumulative capacity >2 Ah/cm², **Figure 7c**). This corresponds to high average specific discharge energy and power, amounting to 277 Wh/kg and 550 W/kg, with respect to the cathode mass. For iron-free nickel cathodes, we could demonstrate stable cycling even at 160 mA/cm² (3.2C, 10-90% SOC, >140 cycles, cumulative capacity 6 Ah/cm², **Figure 7c**). During long-term cycling, planar cells with iron-free nickel delivered an average specific discharge energy and power of 258 Wh/kg and 1022 W/kg, with respect to the cathode mass. This represents 400% improvement in specific power, compared to the best performing planar sodium-metal chloride cells reported in literature [41], while simultaneously increasing the specific energy by 74%. Our study further provides important insights on the evolution of internal cell resistance, leading to the progression of separate reaction fronts for the different electrochemical reactions in the cell (e.g. $Fe/FeCl_2$, $Ni/NiCl_2$).

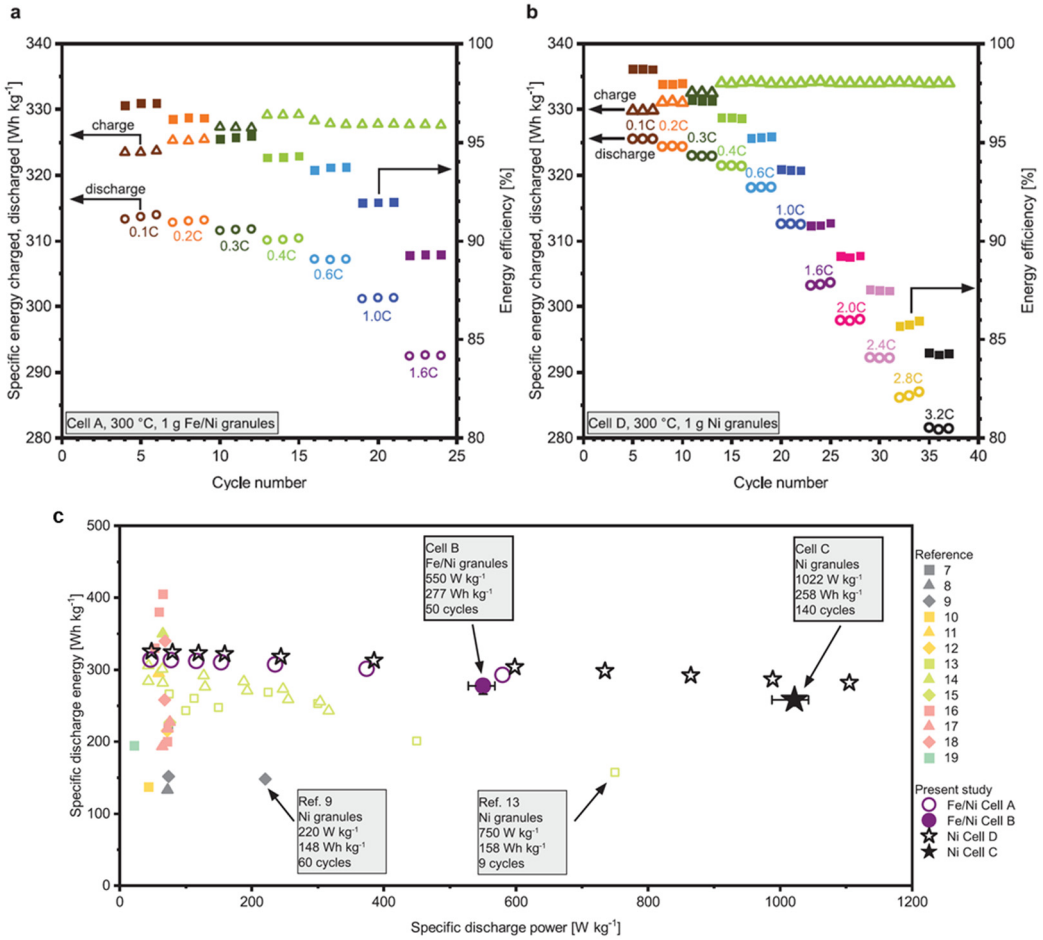

Figure 7 Planar prototype full cells with **50 mAh cm⁻² cathode loading** at 300 °C. Rate test of a) Fe/Ni cathode granules and b) Ni cathode granules. c) Ragone plot showing specific discharge energy versus specific discharge power of the present study, as compared to literature. Source: [Graeber2021].

In order to increase the cathode loading in the planar prototype cells to that of state-of-the-art tubular cells, we then developed a number of additional passive cell components to manage the (partially) molten and corrosive materials in the cells. With specifically designed coated, corrugated anode current collectors, we achieved stable cycling of state-of-the art Fe/Ni cathodes at a **cathode loading of 150 mAh/cm²**, and at discharge current densities of up to 80 mA/cm² (**Figure 8a**, C/2, 10-100% SOC, 52 cycles, cumulative capacity >7 Ah/cm²). This represents both the highest cathode loading and the highest cumulative capacity cycled in planar high-temperature cells, according to current literature. Careful analysis of the cell potentials at different discharge rates further provides a breakdown of the planar cell resistance, clearly separating the contributions of active and passive cell components at low and high cathode loadings (**Figure 8b**). Compared to the lower cathode loading (50 mAh/cm², <1 Ω), the cell resistance during discharge increased only slightly for the higher loading (150 mAh/cm², <2 Ω). At the same time, we were able to activate a wider capacity window, now ranging from 10% to 100% SOC. As a result, the discharge energies obtained with the higher cathode loading are even higher than previously reported (**Figure 8c**, 300 Wh/kg at 80 mA/cm², with respect to the cathode mass). Furthermore, charge times for 10-100% SOC are below 8 h for this cell (**Figure 8d**, charge current density 20 mA/cm² to 2.68 V). The planar prototype cells with 150 mAh/cm² cathode loading also support charge times below 5 h for 10-90% SOC, as shown over 10 cycles an increased charge current density of 25 mA/cm² at an upper cut-off voltage of 2.72 V (**Figure 8d**).

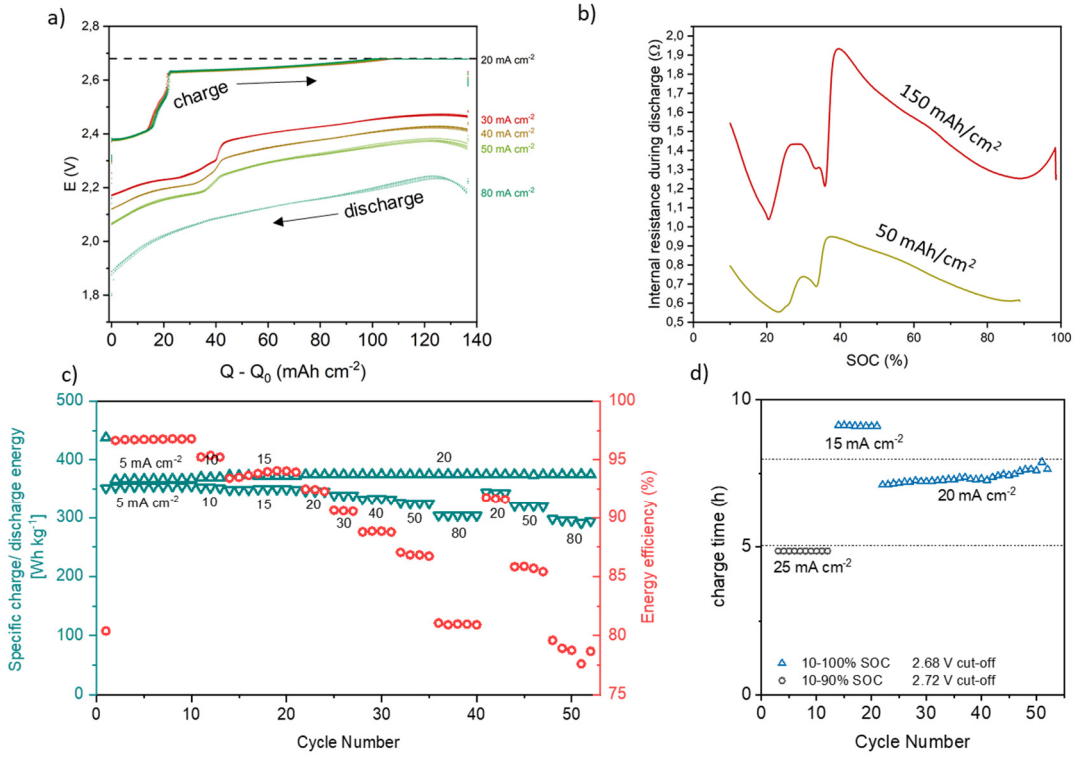

Figure 8 Planar prototype cells with Fe/Ni cathode at **150 mAh cm⁻² cathode loading** at 300 °C. a) Stable voltage curves at discharge current densities between 20 and 80 mA cm⁻² are used to extrapolate the effective cell resistance. b) Comparison of discharge resistance for planar Fe/Ni prototype cells with 50 mAh cm⁻² and 150 mAh cm⁻² cathode loading. c) Rate test and d) charge time for Fe/Ni cathode with 150 mAh cm⁻² cathode loading. Source: [Lan2022a].

The experimental results were then used as input in a **numerical model** to enhance the understanding of relevant processes during cell cycling *[Gutierrez2022]*. A 1D model was developed for planar Na-$NiCl_2$ cells with 50 and 150 mAh/cm^2 cathode loading. A schematic representation of the model is shown in **Figure 9**. This initial model considers only nickel as active metal in the positive electrode. The addition of iron could be considered at a later stage. The model allows for the computation of the cell's electric potential at different states of charge, see eq. (1).

Anodic and cathodic activation losses, $\eta_{a/c}$, are determined through the Butler-Volmer equation, which considers changes in volume fraction of $NiCl_2$, ε_{NiCl2}, during charge and discharge, see equations (2)-(4). It is observed that the values of the exchange current density, $i_{0,Ni}$, and the specific surface area, $a_{s,Ni}$, are reduced or increased as the volume fraction of nickel chloride is increased or decreased during the process of charging and discharging, respectively. The exponent p is a semi-empirical factor that considers the shape of Ni particles (around 2/3 for cubical or spherical particles and larger values for filamentary particles). Notice that the exchange current density follows an Arrhenius type behavior regarding the changes on the operating temperature, T. For the ohmic losses, η_{ohm}, we considered only Ohm's law for the lower cathode loading (simplification proposed in a 2D model of tubular Na-$NiCl_2$ cells[42]), while for the higher cathode loading we additionally considered variations in the concentration of the melt composition ($\nabla\, c \neq 0$), see eq. (5). In both cases, we assumed the same initial volume fractions and specific surface area of Ni as displayed Figure 9.

(1) $$V = E^{o}_{eq} + \eta_a - \eta_c + \eta_{ohm}$$

(2) $$i_{Ni} = i_{0,Ni} a_{s,Ni} \left(e^{\alpha_a \frac{F}{RT}\eta} - e^{-\alpha_c \frac{F}{RT}\eta} \right)$$

(3) $$i_{0,Ni} = i_{0,ref,Ni} \varepsilon_r{}^{p} \exp\left(-\frac{E_A}{R}\left(\frac{1}{T} - \frac{1}{T_{ref}}\right)\right) \begin{cases} \varepsilon_r = \frac{\epsilon_{NiCl_2,max} - \epsilon_{NiCl_2}}{\epsilon_{NiCl_2,max}} \; (i > 0) \\ \varepsilon_r = \frac{\epsilon_{NiCl_2}}{\epsilon_{NiCl_2,max}} \; (i < 0) \end{cases}$$

(4) $$a_{s,Ni} = a_{s,ref,Ni} \varepsilon_r{}^{p} \qquad (1)$$

(5) $$i_l = -\sigma \nabla\varphi - \frac{2\sigma RT}{F}\left(1 + \frac{d\ln f}{d\ln c}\right)\left(t_+ + \frac{c}{c_0}\right)\nabla \ln c$$

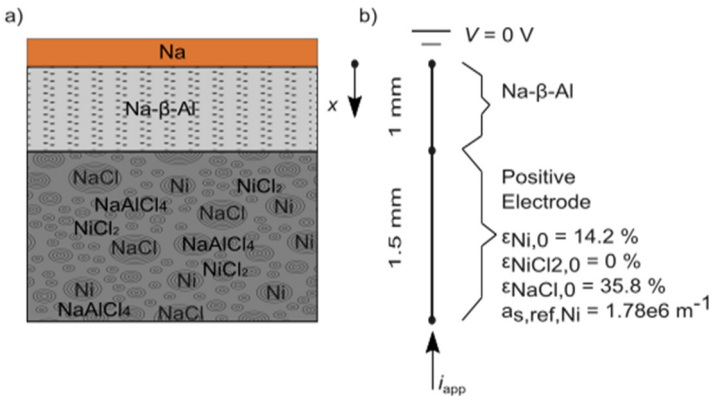

Figure 9 (a) Schematic representation of cycling of a planar Na-$NiCl_2$ cell and its main components. (b) Model dimensions, most important boundary conditions (50 mAh/cm^2), and initial volume fractions and specific surface area of nickel.

To validate the model, we compare numerical and experimental results from *[Graeber2021]* for a cathode loading of 50 mAh/cm^2 in **Figure 10a**. In order to simulate a cathode loading of 150 mAh/cm^2 from *[Lan2022a]* (**Figure 10b**), variations in the concentration of the salt melt were taken into account ($\nabla c \neq 0$, ionic transport number $t(Na^+)$= 0.85, initial concentration c_0= 34 M upon charge, c_0= 0.9 M upon discharge). Generally, the numerical results are in good agreement with the experimentally determined magnitude of the electric potential. Also, the shape of the potential curves' changes as a function of the state of charge agree. The potential initially stays almost constant and then rapidly changes when the battery is almost fully charged or discharged. These fast changes are attributed to the changes in the volume fraction of the $NiCl_2$ phase in the positive electrode. During discharge, the difference between experimental and numerical results tends to be larger than during charge, in particular for a current density of 3 mA/cm^2. This difference may come from the selection of kinetic parameters (e.g., $i_{0,Na}$, $\alpha_{a/c}$, p, $i_{0,ref,Ni}$) that fitted best the experimental results at a current density of 20 mA/cm^2. For the rest of the results the small variation in voltage may be due to additional ohmic losses that were not considered in the model (contact losses, small variations in concentration of the salt). Furthermore, underestimation of the ionic transfer number, or the use of average properties to represent the whole porous electrode (exponent p) may play a role.

The model supports the hypothesis that the reaction front occurs first at the interphase between the solid electrolyte (Na-β"-alumina), solid cathode active materials (Ni, NaCl), and the molten electrolyte ($NaAlCl_4$). The model also agrees well with the final volume fraction at the end of the charging. Small variations of the final volume fraction with respect to the experimental values (difference of 2.2% for NaCl and 1.3% for $NiCl_2$) may be due to irreversible reactions of additives and aluminum, which were not considered in the numerical model.

This model can predict the electrical voltage during charge and discharge, can help in identifying the main voltage losses, can increase the understanding of the local consumption/formation of species within the battery, and even allows to analyze the temperature distribution within the battery.

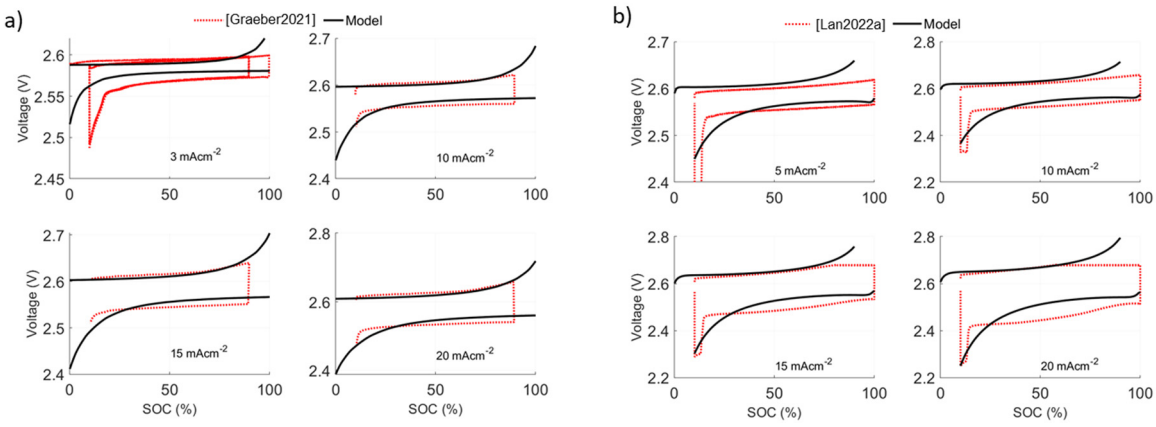

Figure 10 Comparison of the experimental and numerical electrical potential of planar Na-$NiCl_2$ cells as function of SOC for different current densities. Planar cell with a) 50 mAh/cm^2 and b) 150 mAh/cm^2 cathode loading. While the model considers only Ni (30% active metal content) and NaCl, the experimental results with Fe-free granules contain 4.4 wt% additives and 0.5 wt% Al. Furthermore, an upper cut-off potential of 2.68 V is applied in the experiments, which is not included in the model.

3.2 WP2: Large, planar Na-β"-alumina electrolytes

Within the HiPerSoNick project, a multistep process consisting of tape casting, punching, lamination, and sintering was developed to prepare large diameter Na-β"-alumina (> 11 cm, 95 cm^2) [*Ligon2020b*]. As an alternate route to produce Na-β"-alumina electrolytes, the Na_2O vapor phase conversion of α-Al_2O_3/YSZ to Na-β"-alumina/YSZ was explored. Na_2O vapor converted Na-β"-alumina materials were found to be stronger but less conductive than Na-β"-alumina composites with the same YSZ content [*Ligon2020a*]. Due to the significantly better ion conductivity of sintered samples, we focused on preparing pilot electrolytes by sintering, instead of vapor phase conversion in the HiPerSonick project.

Additionally, we introduced uniaxial pressing of spray granulated powder as an alternative process for the production of large Na-β"-alumina discs, which reduces the debinding step during sintering. To assure mechanical integrity, flatness, and reproducible preparation of planar electrolytes, we further enhanced the processing and sintering procedures *[Kovalska2022a]*.

The composition of the resulting Na-β"-alumina electrolytes, prepared by both tape casting and uniaxial pressing, corresponds to that of state-of-the-art tubular electrolytes, comprising 9.7 ± 0.2 wt% Na_2O. The optimization of repeatability conditions was improved in the third year of the project. Na-β"-alumina discs produced by the uniaxial pressing method had a diameter of 111.3 ± 0.2 mm after sintering, and were machined to a thickness of 1 ± 0.2 mm (**Figure 11**). The average value was calculated from 15 samples. The uniaxial pressing method can also be applied as part of large-scale production, by which a 1 mm sample thickness of is achievable without any machining using a floating die press system. For the tape casting method, batches of 400 g slurry were prepared, from which about 4 meters of tape were produced, resulting in 30 discs with a diameter of 140 mm and a thickness of 250 µm. In order to sinter a 1 mm thick Na-β"-alumina disc, 8 - 10 tape discs where stacked together. Thus, about 3 to 4 samples with a diameter of 109.0 ± 0.3 mm were prepared from one slurry batch, where the average value presented was calculated from about 28 tape cast samples. The final product of Na-β"-alumina electrolyte produced by both methods has a flexural strength of 226 ± 13 MPa, an ionic conductivity of 0.19 S/cm at 300 °C, and a density of 97 %, thus fulfilling the requirements for a battery electrolyte.

The impact of sintering conditions and structural reinforcement by zirconia addition on flexural strength and ion conductivity were previously studied in the CTI/Innosuisse project Sonibat (completed in 2018). A joint paper was published with FZSoNick on the influence of sintering conditions on microstructure and ion conductivity of Na-β"-alumina [*Bay2019*]. By adding 5 vol% zirconia particles, the fracture strength of electrolytes is increased to > 200 MPa, from ~ 160 MPa of pure Na-β"-alumina. However, addition of zirconia also decreases the conductivity of the electrolyte, e.g. from 0.19 S/cm to 0.16 S/cm at 300°C [*Bay2020*]. Within the HiPerSoNick project, we further studied the influence of processing on

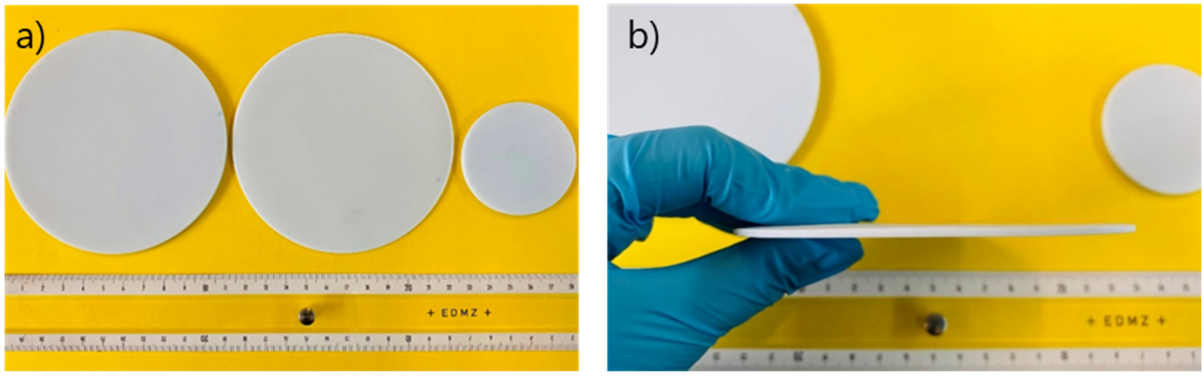

Figure 11 a) Na-β"-alumina ceramic disc prepared by uniaxial die pressing, diameter 111.3 ± 0.2 mm; b) Na-β"-alumina ceramic disc prepared by tape casting, diameter 109 ± 0.3 mm.

Na_2O evaporation and phase content of Na-β''-alumina ceramics. In this context, we presented a method to estimate the Na_2O content in the crystal structure of Na-β''-alumina from the c-lattice parameter, which may be applied in the production of planar electrolytes of large area in the future [*Bay2021*]. Furthermore, an extensive data set on ion conductivity of Na-β''-alumina ceramics, prepared under variable processing conditions during both the Sonibat and the HiPerSoNick projects, enhanced the understanding of solid ion conductors in general. We identified a linear relation between activation energy and conductivity at a given temperature, which we could relate to grain size effects in materials with highly resistive grain boundary phase in general [*Heinz2021*]. Furthermore, this study confirmed the good quality of Na-β''-alumina ceramics applied in this project, enabling its application not only at high temperatures (0.2 S/cm at 300 °C), but also at room temperature (> 10^{-3} S/cm).

Integration of the large, planar Na-β''-alumina electrolytes into battery cells requires their sealing to insulating α-alumina collars, to form the ceramic subassembly. The pilot cells developed in this project are based on α-alumina collars, for which we specified the geometry and dimensions displayed in **Figure 12** (L-shape step design). When selected in the marketplace, industrial suppliers of ceramic components typically provide tolerances of ± 2% or ± 0.2 mm (whichever is greater), which we included in the specifications. In this design, the planar Na-β''-alumina electrolyte is placed on the step between middle diameter (MD, 113 ± 1 mm) and inner diameter (ID, 102 ± 1 mm) .

To provide these pieces through the course of the project, we ordered three batches of α-alumina collars of 10 pieces each from Almath crucibles ltd, a small British manufacturer and global exporter of alumina crucibles and ceramic refractory products. Almath produced the α-alumina collars by a cost-efficient combination of slip casting and machining. The tolerance of delivered collars was within the range of specifications (outer diameter OD = 122.5 ± 0.5 mm; MD = 112.3 ± 0.3 mm; ID = 101.7 ± 0.2 mm; total height H = 30.1 ± 0.2 mm; lower height LH = 14.2 ± 0.2 mm). However, delivery was significantly delayed for all batches, as preparation of the collar geometry turned out to be more difficult than anticipated. As a result, Almath increased the price of α-alumina collars, from 55 GBP per piece in the first order, to 75 GBP and 105 GBP per piece in the second and third order.

When placing the Na-β''-alumina electrolyte inside the α-alumina collar, the sealing gap between them has to be filled with the glass sealant in order to join it and form a hermetic seal. The average calculated gap length between the uniaxial pressed electrolytes an the collar wall (MD) was 0.5 ± 0.1 mm, and between tape-cast electrolytes was 1.5 ± 0.1 mm. The planar step width (SW) of the collars was 5.2 ± 0.2 mm. Thus, the seal width, corresponding to the overlap of Na-β''-alumina discs and step width of the collars, amounts to 4.7 ± 0.1 mm for uniaxially pressed samples, and 3.7 ± 0.1 mm for tape-cast samples.

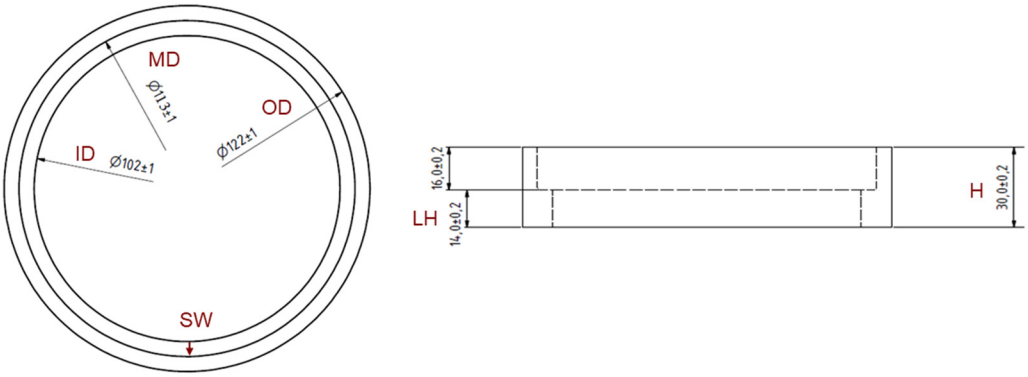

Figure 12 Geometry and dimensions of α-alumina collars for pilot cells (outer diameter OD= 122 ± 1 mm; middle diameter MD= 113 ± 1 mm; inner diameter ID= 102 ± 1 mm; total height H= 30 ± 0.2 mm; lower height LH= 14 ± 0.2 mm; step width SW).

Furthermore, the typical tolerances accessible by slip casting at these dimensions negatively affected the management of molten phases at the electrodes during pilot cell cycling. To obtain α-alumina collars with tighter tolerances, we also ordered from the Swiss company Metoxit AG, who offered to produce the pieces by powder pressing and green machining at a price of 630 CHF/pc (batch of 10 pieces). With a delivery time of 3 months we received this batch of α-alumina collars with improved tolerances (OD = 121.8 ± 0.2 mm; MD = 112.4 ± 0.2 mm; ID = 101.5 ± 0.2 mm; H = 30 ± 0.06 mm; LH = 14 ± 0.04 mm). As we expect a prolonged cycle life of pilot cell with these new α-alumina collars, we will continue our experiments with pilot cells at Empa also beyond the HiPerSoNick project, and plan to include the results in an upcoming publication.

3.3 WP3: Sealants

The processing and functionality of glass sealants is vital for enabling a long lifetime of Na-$NiCl_2$ battery cells. The glass seal between Na-β''-alumina and α-alumina insulator (**ceramic-to-ceramic**) is a significant challenge, even for small cells. Seal failures contribute a significant fraction to the overall scrap rate in the lab and during production. Sealing is even more challenging for planar pilot cells, where a tight hermetic seal between Na-β''-alumina and α-alumina is required along the much longer sealing path, compared to tubular cells. Thus, fine-tuning the coefficient of thermal expansion (CTE), the bonding behavior, and the proper composition and amount of glass sealants is of high importance.

In the production of tubular cells at FZSoNick, the thermo-compression bond applied to seal the α-alumina insulator to a metal current frame (**ceramic-to-metal**) contributes a significant cost. We thus also investigated the possibilities for joining a metal cell case to a ceramic insulator with glass seals, replacing thermo-compression bonding. Ideally, both glass seals (ceramic-to-ceramic and ceramic-to-metal) could be applied in a one-step process. While the planar pilot cells developed for battery cycling in this project are based on heavy steel endplates, we also investigate sealing solutions for a cell housing with state-of-the art battery components such as nickel-plated steel (Hilumin). In this context, the ceramic-to-metal seal developed in WP3 is instrumental for replacing the bolted steel endplates of planar lab pilot cells by a commercially viable design, capable of cycling in ambient atmosphere.

In a first phase of the project, we **screened** a variety of commercially available glass sealants that could be applied for ceramic-to-ceramic and ceramic-to-metal seals. The selection of the glass was based on their studied and previously reported gas-tightness and mechanical stability. We focused on investigating the nature of adhesion, composition, structure, and corrosion resistance of selected commercial glasses (Schott G018-266 and Schott G018-402) in dedicated experiments, and compared their performance to the glass sealant employed for ceramic-to-ceramic seals in state-of-the-art tubular cells at FZSoNick *[Kovalska2022b]*.

In order to comprehend the properties of glass for subassembly cell, we investigated slurry preparation, deposition capability, sintering temperature, and properties of the solid glass. Thermo-physical analysis of the cured glass crystallization allowed to distinguish the surface nucleation process for each of the selected and analyzed glasses. The results of the thermo-physical and structural analysis performed by TG/DSC and X-ray diffraction indicated the possible range of curing temperatures. Corrosion tests were performed on cured cut pieces of a glasses immersed in $NaAlCl_4$ during 21 days at 350°C to assure no mass loss occurred in this environment. Based on these studies, we conclude that the curing temperature of FZSoNick's ceramic-to-ceramic glass seal can be reduced from currently 1010 °C to 980 °C for ceramic-to-ceramic seals. The same composition is also suitable to seal ceramic-to-metal, but this requires temperatures >1000 °C in order to assure suitable surface wetting. Apart from FZSoNick's glass seal, two commercial products (Schott G018-266 and Schott G018-402) were identified as suitable for sealing applications in Na-$NiCl_2$ cells.

To prepare ceramic subassemblies for pilot cells (**Figure 13**), sealing of planar Na-β''-alumina electrolytes to α-alumina collars (both from WP2) was mainly performed with standard FZSonick glass (**ceramic-to-ceramic**). The glass sealant was deposited on the L-shaped collar rim, where it was cured at 1010 °C (standard temperature program from FZSoNick). The quality of the sealed subassembly was tested by an isopropanol penetration test, and in case of leakage was sealed a second time. In total, more than 20 samples were sealed at the standard temperature of 1010°C, and 2 subassemblies were sealed at a lower temperature of 980 °C, as suggested by our studies above. Also, sealing was successfully performed with Schott G018-402 at 960 °C (2 samples) and G018-266 at 780 °C (2 samples). To evaluate the mechanical stability and thermal stress resistance of the ceramic subassemblies, we performed a heat cycling test (100 cycles at a high heating rate of 600 °C/h between room temperature and 350 °C). All subassemblies passed this test, and no cracks or damage was

observed on the Na-β''-alumina electrolytes or sealing layers. Also, we compared the cross section of the sealed planar subassembly with that of a tubular cell sealed at FZSonick, where we could observe sealing thickness (688 mm) and sealing defects (**Figure 14**).

A suitable design of a cell housing using light-weight end caps made from Hilumin sheet metal is presented in **Figure 15a**. To respect the thermal stability of the cathode materials, a Hilumin metal ribbon is first sealed to the α-alumina collar (**Figure 15b**). Then, the cathode material is filled in, and the metal cell case is closed by laser-welding. To demonstrate the sealing properties of Schott G018-402, G018-266, as well as FZSoNick's glass seal for **ceramic-to-metal** joining, we investigated the bonding capabilities of α-alumina with two different Hilumin qualities (0.2 mm and 0.6 mm thick). Hilumin is commonly used for cell housings in the battery industry, both for tubular Na-$NiCl_2$ and Li-ion batteries. It is made from steel of variable thickness, which is electrolytically plated with a ~2 µm thick nickel coating. In this project, we investigated the effect of Hilumin thickness, curing temperature, and curing atmosphere (vacuum, argon gas and ambient air) on the quality of ceramic-to-metal seals. The studies showed that oxidation of the metal increases its diffusion into the glass with the formation of a new phase, which increasing the bonding possibilities. The joining of Hilumin (0.2 mm) to ceramics using FZSonick glass in ambient air was successful at 960 °C, while higher temperatures increased diffusion and oxidation as well as damage of Hilumin . The same behavior was observed for Schott sealants. However, the 0.6 mm thick Hilumin required higher temperatures for oxidation and partial diffusion, therefore joining is more difficult. In addition, the shape of the materials being joined plays a role in the possible additional compression that overlaps the CTE mismatch.

The sealing of Na-β''-alumina electrolyte and α-alumina insulator (ceramic-to-ceramic), as well as the α-alumina insulator and metal case (ceramic-to-metal) in a one-step process can be directly linked to the studies of metal-ceramic joining (**Figure 16**). The joining as one step was demonstrated at 980 °C and 1010 °C for small samples of 0.2 mm Hilumin, which were joint to α-alumina, while simultaneously sealing α-alumina to Na-β''-alumina. Sealing was not possible for 0.6 mm Hilumin at these temperatures, but could be feasible after further research.

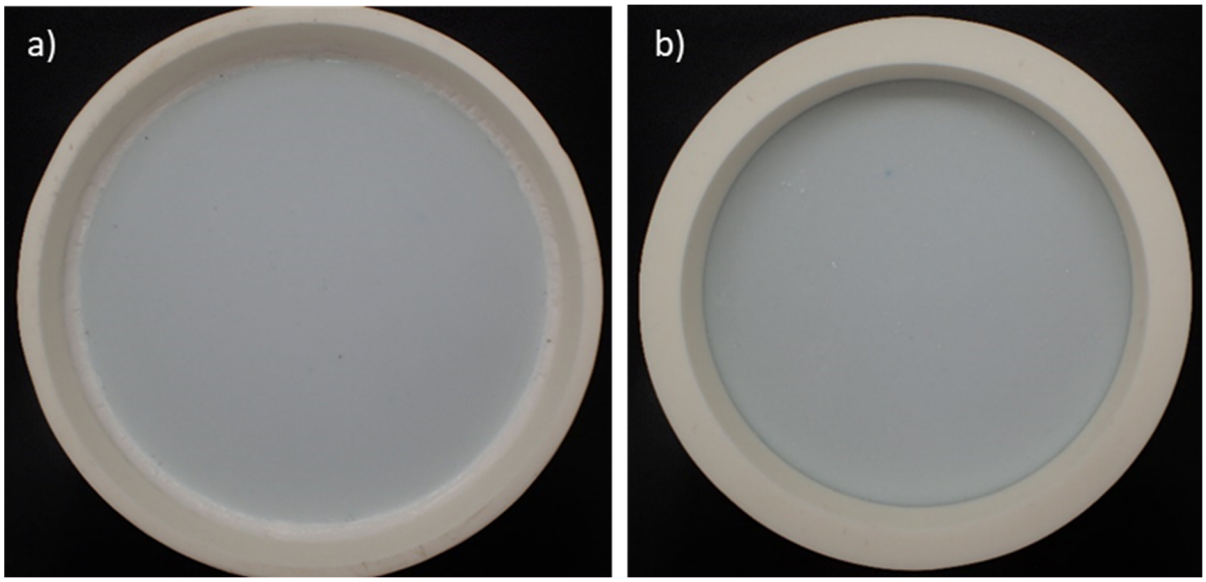

Figure 13 Ceramic subassembly for pilot cells, sealed with FZSonick glass. a) Top view on upper compartment, b) bottom view on lower compartment.

To summarize the activities in WP3, the selected Schott G018-402 and Schott G018-266 glasses can be used for ceramic-to-ceramic sealing as well as for ceramic-to-metal sealing. Studies of the FZSonick glass seal have shown that its sealing temperature can be reduced from 1010°C to 980°C, and that it tolerates thermal shocks in heat cycling test after curing at both temperatures.

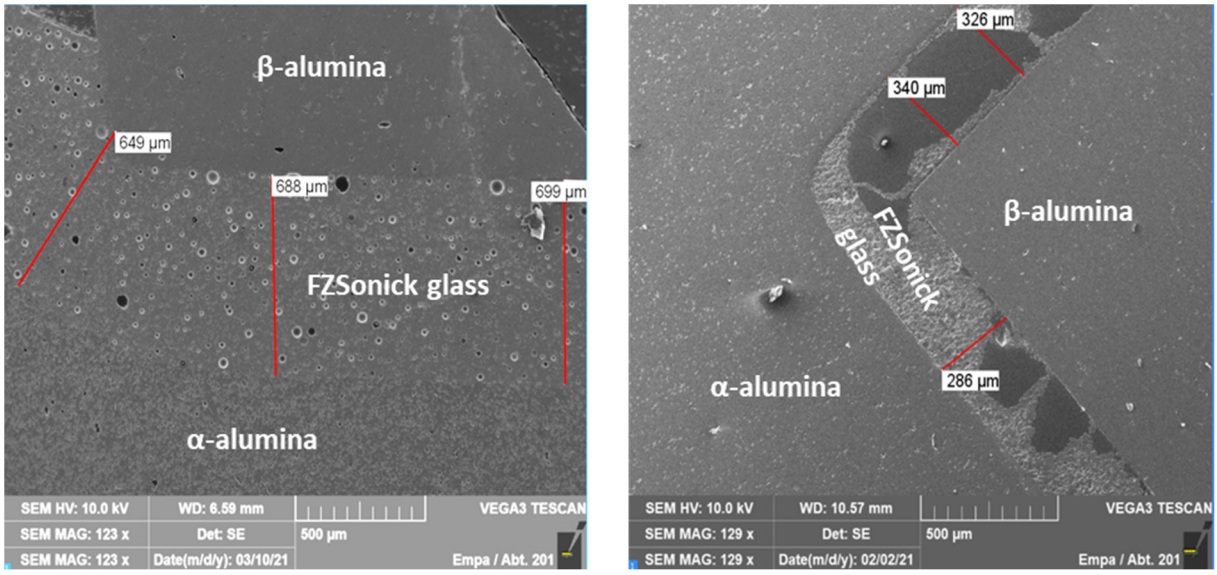

Figure 14 SEM images of ceramic-to-ceramic seals (FZSoNick glass) in ceramic subassembly of a) planar and b) tubular cells.

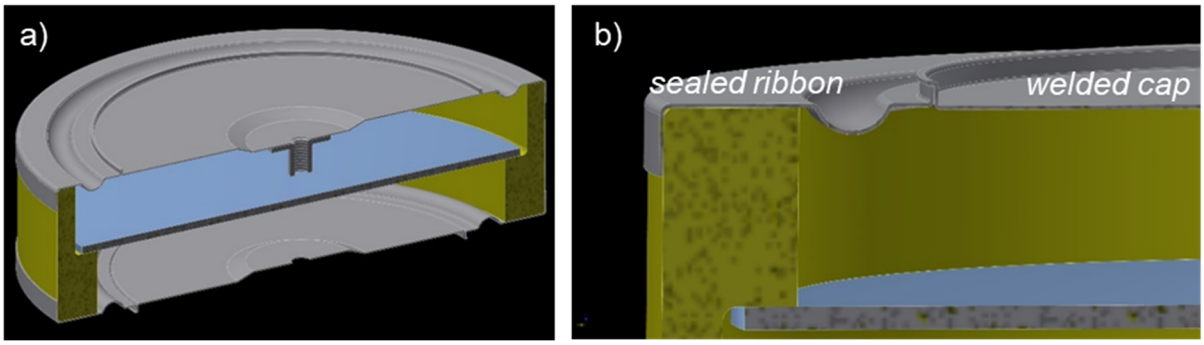

Figure 15 a) Design of cell housing with Hilumin end caps. b) First, an L-shaped Hilumin ribbon is sealed to the α-alumina collar. After filling of the cathode material, a planar Hilumin end cap is laser-welded to the ribbon to close the cell.

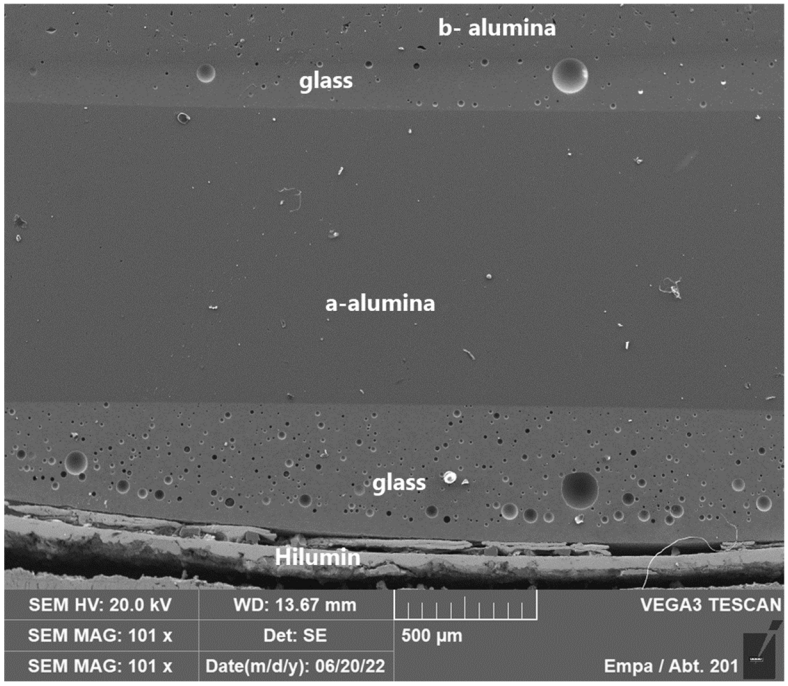

Figure 16 One step joining of Na-β''-alumina to α-alumina to Hilumin (0.2 mm) at 980 °C.

3.4 WP4: Cathode development

Independent of the cell geometry, modifications to the cathode composition offer great potential to reduce the manufacturing costs of Na-$NiCl_2$ batteries. Also in terms of rate capability during charge and discharge, the Na-$NiCl_2$ cathode provides extensive design possibilities. However, for an efficient cathode performance, both composition and microstructure of all components need to be carefully balanced. This is of particular importance as typical Na-$NiCl_2$ cathodes are orders of magnitude thicker than common cathodes in Li-ion batteries, e.g. ~6 mm instead of ~0.1 mm. Thus, highly efficient transport of all necessary ions and electrons is required at all SOC. In state-of-the-art Na-$NiCl_2$ cathodes, percolating nickel particles serve not only as active materials, but also constitute an electronically conductive backbone. All cathode materials (in the maiden state: the active metals Ni, Fe, and Al; NaCl; additives) are immersed in a molten, secondary electrolyte ($NaAlCl_4$), which provides fast ion transport through the 3D cathode structure. Thus, to enable fast cycling rates, processing of the cathode needs to provide a microstructure, which balances both electronic percolation in the nickel backbone and ion transport through molten $NaAlCl_4$ at all SOC. Such high degree of microstructural control can be achieved by combination of suitable powder morphologies (e.g. filamentary Ni255) and carefully tuned granulation of the cathode powders.

One ambitious project target was to increase the ratio of nominal cell capacity over mass of nickel in the cathode to 0.4 Ah/g, corresponding to a reduction from 125 g to 100 g of nickel in a cell with 40 Ah capacity. Detailed experimental series were performed, both applying an established lab granulator, and the production equipment at FZSoNick (several kg batch size in both cases). In the course of the project, we continuously adopted the granulation process, in order to obtain suitable microstructures for the different compositions.

In a first experimental series, we adopted the cathode processing to decrease the nickel content of the cathode (125 g per cell) by -4 g Ni, -6 g Ni, and -9 g Ni (**Table 3**). To characterize these cathode formulations, the resulting granules were re-introduced to the state-of-the-art production flow of tubular cells (cathode loading ~150 mAh/cm^2), including professional sealing. For the first series, we applied dynamic stress tests (Figure 2) to compare the performance of cell modules with standard composition reduced nickel content. However, with this procedure, no significant degradation was observed in the reference discharge curves of the tubular cells before and after 50 DST blocks (1 month of testing, **Figure 17a,b**). The discharge energy during the reference discharge over the nominal capacity of 38 Ah remains constant for all samples (**Figure 17c**).

While the DST protocol represents an accepted accelerated aging test to define cycle life and battery performance for automotive applications, the frequent but short power pulses applied in the DST procedure during discharge and regeneration (e.g. 8 s discharge pulse at 130 W, up to 310 mA/cm^2) are far away from typical load profiles of Na-$NiCl_2$ batteries. Indeed, our analysis indicates that longer pulses at lower current have more severe effects on the cathode performance than the short pulses applied during DST cycling. Therefore, for the long-term cycling of tubular pilot cell modules in WP5.2, we adopted a specific life test procedure developed by FZSoNick for their Na-$NiCl_2$ batteries (Figure 3, and p.41ff). This life test provides more demanding long-term cycling conditions, and is better suited to analyze the ageing of such battery cells.

	standard	-4gNi	-6gNi	-9gNi
Ni [g]	**125**	**121**	**119**	**116**
NaCl [g]	97	97	97	97
Fe, Al, additives [g]	26	26	26	26
total mass [g]	248	244	242	239
total capacity [Ah]	43.1	43.1	43.1	43.1
usable capacity (Ni+Fe) [Ah]	39.3	39.3	39.3	39.3
spec. usable capacity [mAh/g]	159	161	163	164
nom.capacity(40Ah)/Ni [Ah/g]	0.32	0.33	0.34	0.34

Table 3 Cathode compositions with reduced nickel content (-4 to -9 g Ni), prepared in first experimental series.

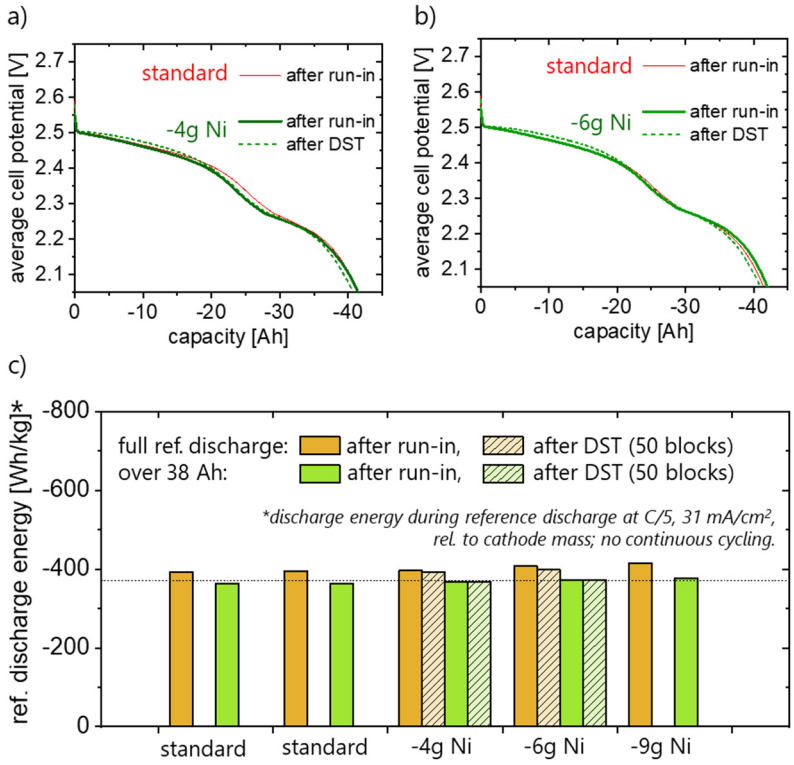

Figure 17 Evaluation of reference discharge curves (at 31 mA/cm^2, lower cut-off voltage 2.05 V), collected before and after 50 blocks of DST cycling (~1 month) for cathode compositions with **a)** -4g Ni, **b)** -6g Ni. **c)** The specific discharge energy of the reference discharge cycles does not change significantly after 50 DST blocks for cathode compositions with -4g Ni and -6g Ni. Similar results were also obtained for all other cell modules (-9 g Ni, 2x standard cathode), but the reference discharge could not be recorded after 50 blocks due to technical problems.

3.5 WP5: Demonstration of planar and tubular pilot cells

3.5.1 WP5.1: Planar pilot cells

To scale up the planar cell design to pilot cells of ~90 cm^2 active area and above, we first performed a series of theoretical studies on the mechanical stability, as well as on the expected weight and volume of the planar design candidates. In a **mechanical analysis** of Na-$NiCl_2$ battery cells [*Heinz2020*] we quantified the volume changes of the electrode materials based on thermal history and electrochemical cell reactions. These volume changes can result in detrimental gas pressure differences between the electrode compartments, which easily exceed the mechanical strength of the brittle ceramic electrolyte in planar cells (**Figure 18**). However, our analysis shows that pressure difference and stress on the electrolyte scale with the gas pressure in the electrode compartment at cell closure. Thus, the volume changes of the electrode materials can be compensated, and cells of large active area >260 cm^2 can be mechanically stable when sealed at a low gas pressure (few mbar). For cells with 90 cm^2 as targeted in this project, a pressure of 10 mbar in both electrode compartments upon cell closure is sufficient.

We further estimated the **potential weight** (and volume) **of planar high-temperature Na-$NiCl_2$ battery cells**, assuming state-of-the-art components and manufacturing equipment (40 Ah cell capacity, 260 cm^2 active area). This reveals that a transition from a tubular to a planar cell geometry generally results in an increase of cell weight and volume. This is caused by the increased contribution of α-alumina insulator, seals, and cell housing, which scale with the circumference of the active cell area in planar cells. A reduction in cell weight and volume is feasible by stacking two (or more) cells (**Figure 19**). However, the development of single planar cells is required first, as stacking could affect the failure mechanisms in Na-$NiCl_2$ batteries, and safe operation needs to be assured.

Based on our experience with prototype cells, we designed and **manufactured planar pilot cells of ~90 cm^2 active area** (**Figure 20**). The corresponding components, comprising end plates, ceramic subassemblies, anode current collectors, cathode current collectors, and fittings are displayed in **Figure 21**. In our pilot cell design, we adopted **a monolithic α-alumina insulator with L-shape profile to** host the large Na-β''-alumina electrolyte discs prepared in WP2. This avoids gas leakage to and from the outside environment at the glass seal (between α-alumina insulator and β''-alumina electrolyte), and reduces the number of glass seals (cost and weight). We designed our end plates to fulfill the sealing conditions of our pilot lab cells: closing the ceramic subassembly in a glovebox at room temperature, as well as applying stiff stainless steel cell end plates, bolts, and temperature resistive graphite seals or metal O-rings, to seal the α-alumina insulator to the metal case. Standard cell assembly procedures developed for both planar prototype and pilot cells in this project are summarized in Appendix A. If planar cells are to be commercialized, thinner end plates (e.g. Hilumin, as applied in state-of-the-art cells) can be applied, and cells can be closed by combining glass seals and welding (as investigated in WP3). We further developed a setup to perform vacuum infiltration of the cathode in pilot cells. Furthermore, we designed and manufactured two custom-made heating cubes for the pilot cells, serving for both vacuum infiltration and pilot cell cycling.

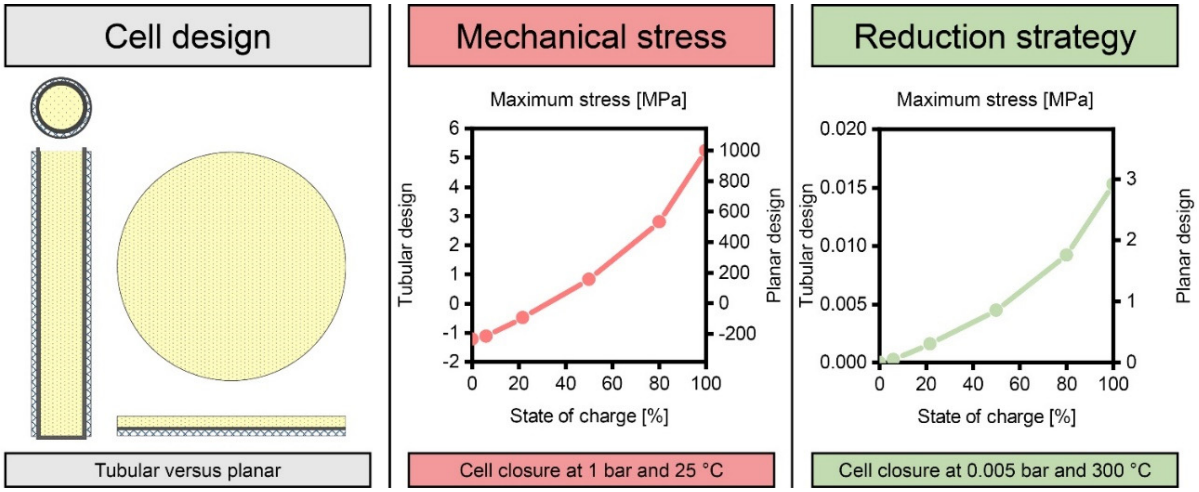

Figure 18 The **mechanical stress** on the ceramic electrolytes is much higher in a planar cell design, compared to a tubular design. However, this can be compensated by sealing the cells at reduced gas pressure. Source: [Heinz2020].

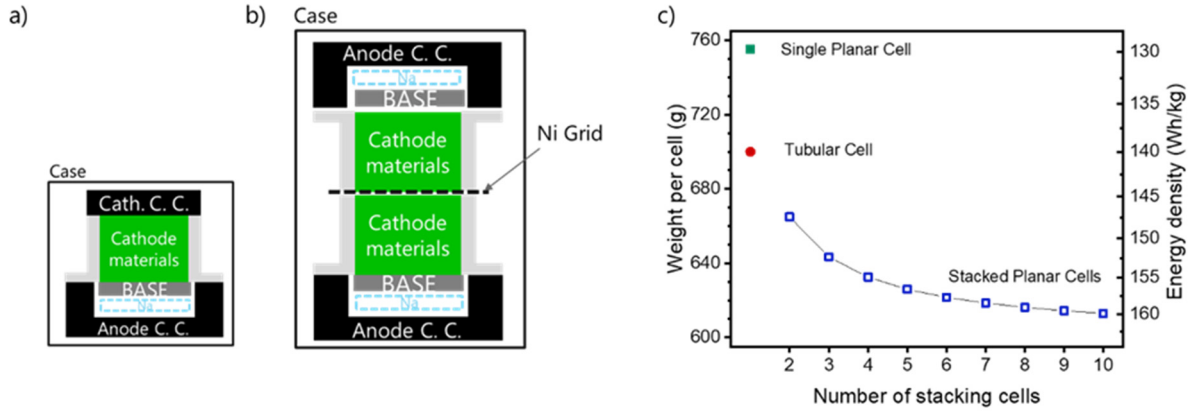

Figure 19 Schematics of planar cell design, including the most important core and supporting components in a) single cell, and b) dual cell stack. c) Projected **evolution of weight and energy density for stacked planar cells,** based on state-of-the-art core components, compared to single planar and tubular cells (40 Ah capacity, 260 cm^2 active area). Source: [Lan2022b].

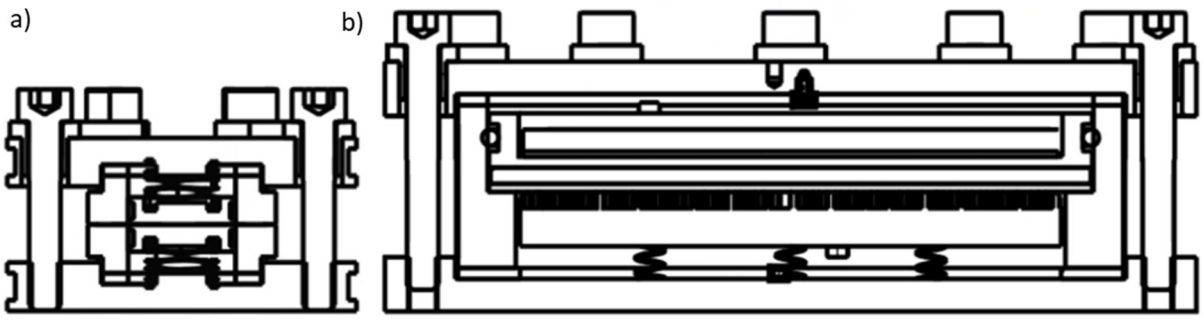

Figure 20 Schematic and size comparison of a) prototype cell (3 cm^2 active area) and b) pilot cell (~90 cm^2 active area) designed in this project. Source: [Lan2022b].

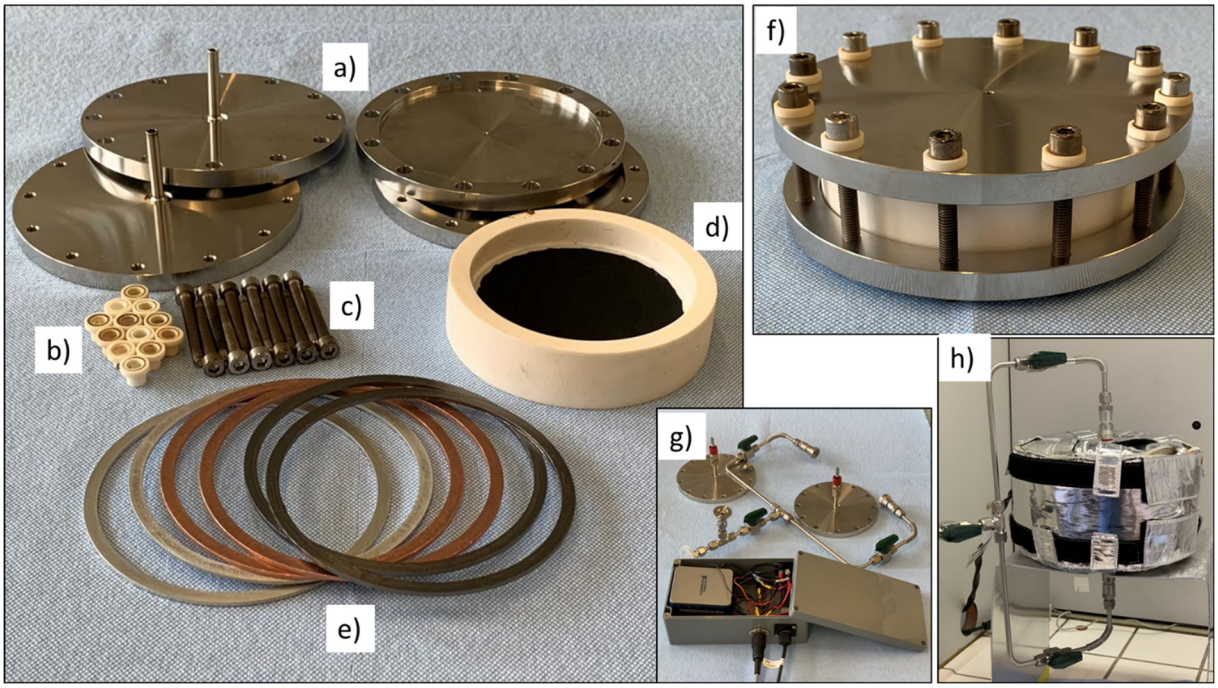

Figure 21 Components and assembly of **pilot cells, ~90 cm^2 active area**. a) Stainless steel bottom and top cell endplates, with two different types. b) α-alumina washers to electronically separate anode and cathode cell caps. c) Screws to bolt the cell. d) Ceramic sub-assembly consisting L-shaped α-alumina collar and Na-β"-alumina electrolyte (with carbon coating). e) Metal and graphite seal (inserted between ceramic sub-assembly and endplates). f) Complete assembly of planar pilot cell. g) Connection system and data collection kit for sealing test between ceramic sub-assembly and endplates. h) Set-up for infiltration of granules by $NaAlCl_4$ in pilot cell cathode. Source: [Lan2022b].

With continuous enhancements of the planar pilot cell design, we successfully performed long-term cycling of a pilot cell at a cathode loading of 80 mAh/cm^2 for >2.5 months in spring 2022. The test was operated between 1.8 and 2.72 V cut-off voltages and 10 to 90% SOC, with various current densities (2-10 mA/cm^2 during charging, 2-20 mA/cm^2 during discharging). Textured anode current collectors were prepared to reduce the loss of sodium during cycling, and the O-rings between the alpha collar and endcaps were improved. However, geometrical variations and dimensional tolerances of the cell components hindered an efficient management of molten materials at the electrodes. During assembly, gaps of up to 1 mm were observed between the ceramic α-alumina collars and the metal current collectors on both electrodes. These imprecise fittings can entail the loss of $NaAlCl_4$ at the cathode, and of molten sodium at the anode. Furthermore, due to the early stage of planar pilot cell development, the passive components added a higher electrical resistance, compared to state-of-the-art components, which reduced the discharge energy and energy efficiency. At the same time, loss of molten materials occurred at the electrodes, which reduced the accessible capacity window. As shown in **Figure 22a**, the cycled capacity was relatively stable during the first ~25 days / 18 cycles, where cycling was performed between almost 10 and 90% SOC. At low charge and discharge rates of 2 mA/cm^2, an energy efficiency of 95% was achieved (**Figure 22b**, cycle 1-2), which reduced to ~88% during cycling at 5-10 mA/cm^2 (cycle 7-56). However, during this time, the accessible capacity decreased continuously during cycling, resulting in a decrease in discharge energy from 290 Wh/kg to >150 Wh/kg, with respect to the cathode mass. Nevertheless, during the following cycles (cycle 57-71) we were able to demonstrate discharge at an increased current density of 20 mA/cm^2, without relevant changes to the degradation profile (energy efficiency 78%). However, due to the limited accessible capacity, the discharge energy decreased further to ~100 Wh/kg. The performance of this pilot cell was thus dominated by insufficient management of molten phases at the electrodes. Furthermore, its rate capability was limited by a relatively high electrical resistance of passive cell components, which again limited the available capacity at the given cut-off potentials (1.8 V and 2.7 V). Nevertheless, at an active area of ~90 cm^2, this data represents the first electrochemical cycling results on large-area sodium-nickel chloride cells. Previous publications in literature had focused on prototype cells of ~3 cm^2 active area (as summarized in [*Graeber2021*]). After demonstrating 71 cycles and transfer of a total cumulative capacity of 304 Ah (3.4 Ah/cm^2, accessible capacity ~60% on average), cycling was stopped due to scheduled re-arrangement of the lab and installation of an extended glovebox.

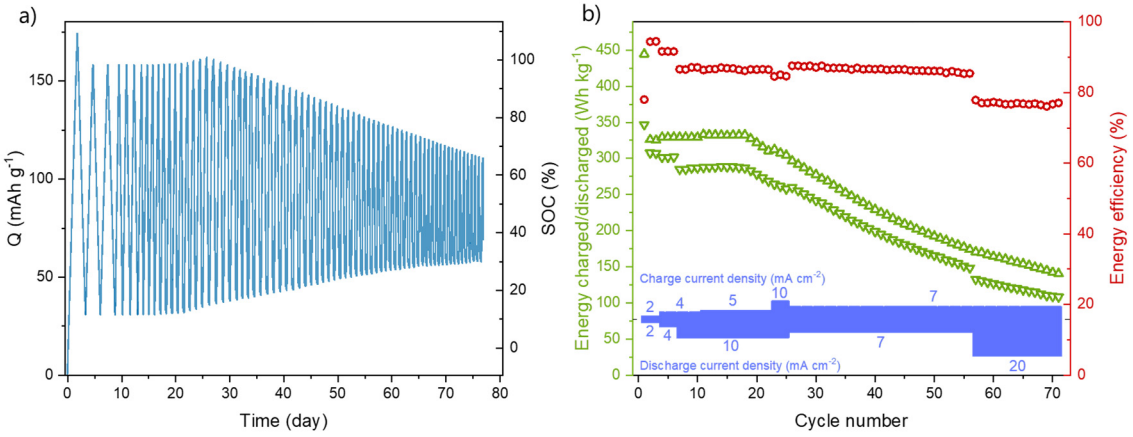

Figure 22 Long-term cycling of **planar pilot cell**, ~90 cm^2 active area, cathode loading 80 mAh/cm^2. Evolution of a) cell capacity with time, and b) charge/discharge energy as well as energy efficiency with cycle number.

3.5.2 WP5.2: Tubular pilot cell modules

Based on the results obtained in WP4, we prepared a second series of enhanced cathode formulations, in which we gradually reduced the nickel content to the target value (-25g Ni, corresponding to 0.4 Ah nominal capacity per gram of nickel). To stabilize the cathode microstructure at reduced nickel content, we enhanced the mixing and granulation process, introduced a new carbon-based additive in some formulations, and additionally increased the aluminum content in another. Most measure aimed at increasing the porosity at the cathode, while maintaining electronic conductivity. The corresponding cathode formulations, which were all applied in tubular pilot cell modules, are summarized in **Table 4**. For each composition, modules comprising 10 tubular pilot cells each were prepared at FZSoNick (**Figure 23**, 2.3-2.5 kg cathode material per module, cathode loading ~150 mAh/cm^2) and characterized by the life test procedure (**Figure 3**).

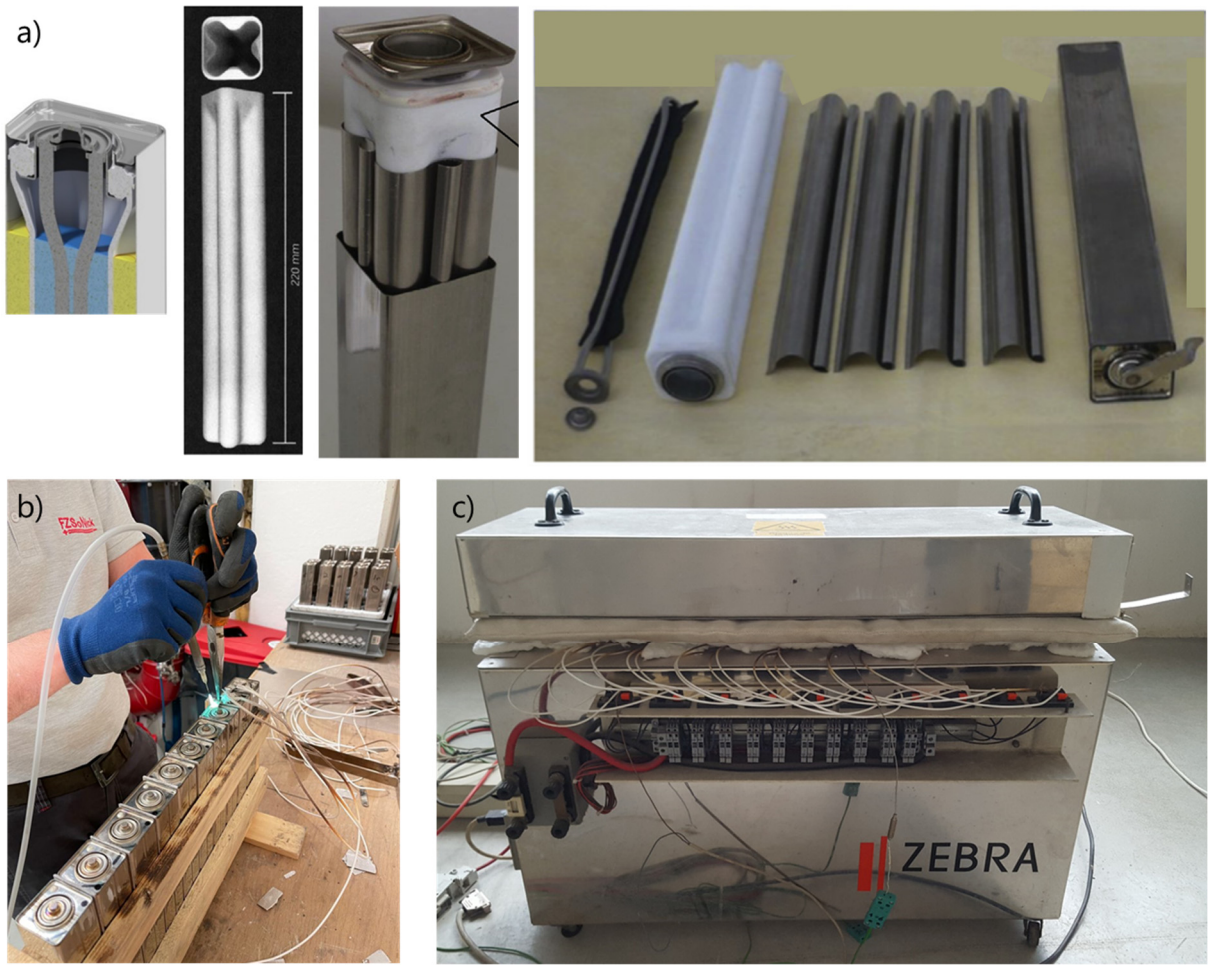

Figure 23 Assembly of tubular cells with modified cathode composition, and their integration into cell modules at FZSoNick, comprising 10 tubular cells. a) Components of state-of-the-art tubular cell, showing tubular ceramic subassembly, shims, cell case, and cathode current collector with carbon felt. Only the cathode formulation is modified in tubular pilot cells. b) Individual contacting of single cells. c) Module with 10 tubular pilot cells in heating unit.

Table 4 Composition and theoretical capacity of **enhanced cathode formulations** developed in this project. Compared to the standard cathode, the nickel content was reduced (up to -25 g Ni), a carbon additive was introduced (up to +2.5 g), and the Al content was increased.

	standard	**-10gNi**	**-10gNi +1.0C**	**-10gNi +2.0C**	**-15gNi +2.0C**	**-25gNi +2.5C**	**-25g Ni +2.5C+0.7Al**
Ni [g]	**125**	**115**	**115**	**115**	**110**	**100**	**100**
NaCl [g]	97	97	97	97	97	97	103
Fe, Al, additives [g]	26	26	26	26	26	26	27
carbon additive [g]			**1.0**	**2.0**	**2.0**	**2.5**	**2.5**
total mass [g]	248	238	239	240	235	226	232
total capacity [Ah]	43.1	43.1	43.1	43.1	43.1	43.1	43.1
usable capacity (Ni+Fe) [Ah]	39.3	39.3	39.3	39.3	39.3	39.3	39.3
spec. usable capacity [mAh/g]	159	165	165	164	167	174	169
nom.capacity(40Ah)/Ni [Ah/g]	0.32	0.35	0.35	0.35	0.36	0.40	0.40

To assess the degradation of tubular pilot cells, we focus on the evaluation of charge time and energy discharged during the life test (**Figure 24**), which are identified as the most significant performance parameters. The enhanced cathode formulations with reduced nickel content not only reduce the weight and cost of materials, they perform even better than the standard cathode. After tailoring the processing, formulations with -25 g nickel provide both a lower charge time, and a higher discharge energy, compared to the standard cathode. After three life-cycle blocks (200 cycles in total, ~4 months), the charge time for 5-100% SOC approaches 12 h for the standard cathode, as well as for some of the enhanced cathodes. However, the optimized formulation with -25 g nickel maintains a moderate charge time of 10.5 h (**Figure 24a**). In terms of discharge energy, most new formulations provide both higher starting values, and slightly lower degradation, compared to the standard cathode (**Figure 24b**). In "fresh" modules, the standard cathode provides a discharge power of 350 Wh/kg, while the enhanced formulation with -25 g Ni + 2.5 g carbon provides almost 390 Wh/kg. A retention of 80% of the discharge power of a standard cathode was considered as end-of-life criterion (280 Wh/kg). To project the service life of the enhanced cathode formulations, we applied linear extrapolation. A high coefficient of determination was achieved for enhanced formulations with -25 g Ni (R^2 ≥0.97), with slightly lower values for most other compositions (R^2 between 0.80 and 0.86). However, extrapolation for the formulation with -10g Ni is not considered meaningful (R^2 =0.60). For the standard cell module, the projected service life then amounts to ~3250 cycles. For the new cathode formulation with -25 g Ni + 2.5 g carbon, tested over 260 cycles, it is 70% higher, amounting to ~5500 cycles. Similar values are also projected for compositions with -10 g Ni. Considering the strenuous conditions of the life test, we consider this to fulfill the project target of a projected service life > 7000 cycles. Based on these results, adoption of a new cathode formulation with reduced nickel content can bring a significant cost benefit for Na-$NiCl_2$ batteries. While the cost reductions from reducing the nickel content itself may be moderate (e.g. -5 $/kWh, at a Ni255 price of 20 €/kg), an increase in cycle life scales directly with a decrease in overall energy costs per cycle. Considering a cost of 295-345 $/kWh for next-generation sodium-nickel chloride battery packs with reduce nickel content at a design life of 7000 cycles, the overall energy costs would reduce to 0.04–0.05 $/kWh/cycle. This corresponds to a reduction by 37%, compared to state-of-the-art tubular cells with standard cathode.

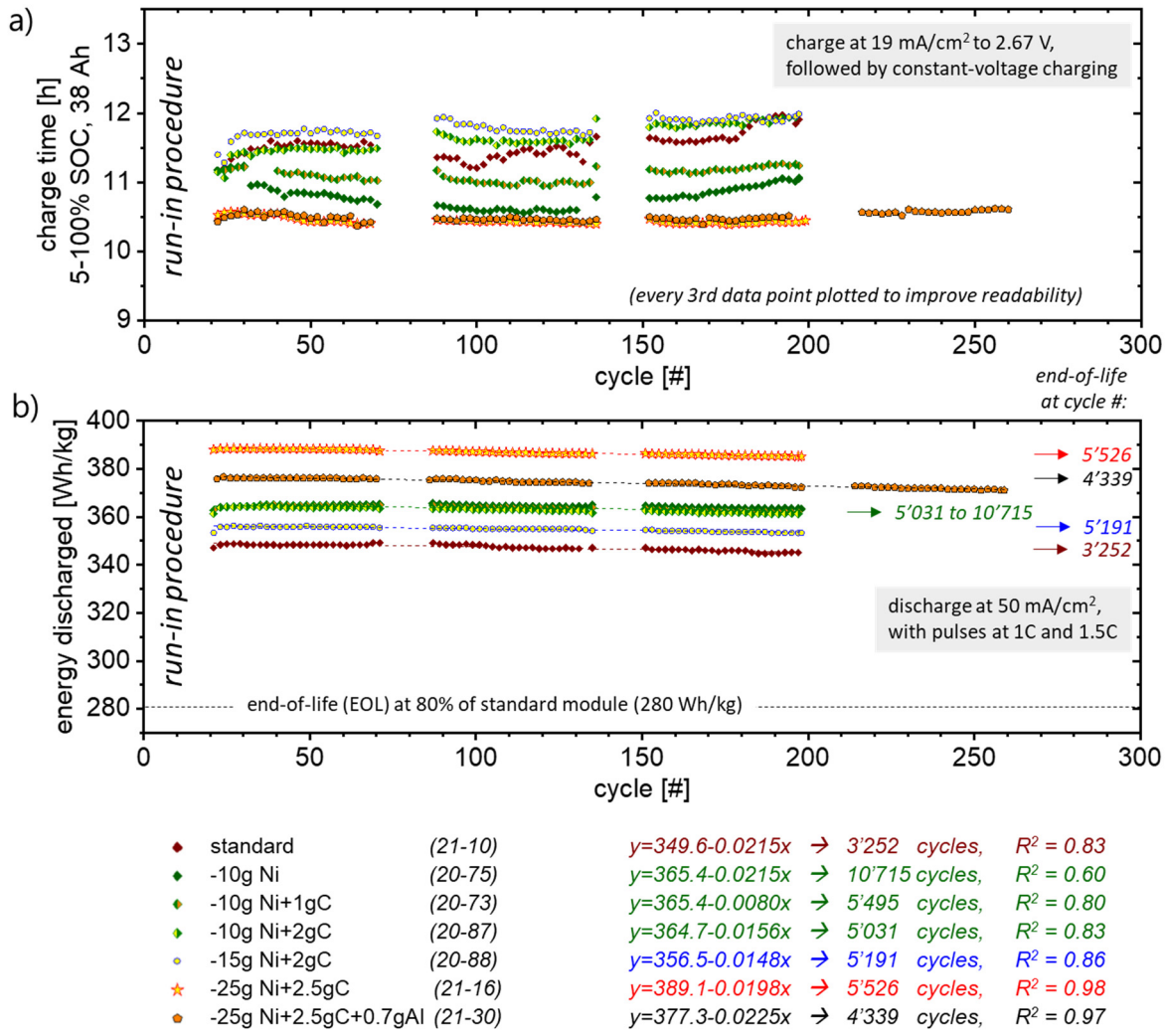

Figure 24 Life test results for tubular cell modules with enhanced cathode compositions, at 270 °C, 5-100% SOC. Evolution of a) charge time and b) energy discharged during. 300 life cycles correspond to a testing duration of ~6 months.

4 Conclusions

The HiPerSoNick project achieved a comprehensive co-development of cell design, electrolyte, sealants, and electrodes for next-generation high-temperature sodium-nickel chloride cells. In addition, it significantly advanced the understanding of the relevant electrode processes, which govern the corresponding electrochemical battery reactions. We identified (i) cell design and (ii) reduction of nickel in the cathode mass to have the strongest impact on battery performance parameters and project targets. Thus, we focused on demonstrating (i) the development planar cells with standard sodium-nickel chloride cathode, as well as (ii) long-term cycling of tubular cells with enhanced cathode formulations and reduced nickel content, both at a relevant cathode loading of ~150 mAh/cm^2.

The **planar cells** (i) developed in this project achieved the highest specific discharge energy reported in literature for planar Na-$NiCl_2$ and Fe-$NiCl_2$ cells so far (>300 Wh/kg, with respect to the cathode mass). They enable successful integration of thick cathodes, demonstrating both the highest cathode loading and the highest cumulative capacity cycled in planar high-temperature cells (> 7 Ah/cm^2).

At pilot scale, the development of scalable planar ceramic electrolytes by tape casting or uniaxial pressing and sintering enabled, for the first time, planar battery cells of up to 90 cm^2 active area. With a total cycling duration of 2.5 months, our best planar pilot cell simultaneously demonstrates the largest cell area and highest capacity cycled in planar sodium-nickel chloride cells so far.

Reducing the nickel content in the cathode (ii) provides a means to reduce both weight and cost of the cathode. We developed enhanced cathode compositions with up to 20% nickel reduction (-25 g per cell, corresponding to 0.4 Ah/g of Ni), enabled by addition of a small quantity of a carbon additive (1-3 wt%). The best cycling performance was achieved with 25 g less Ni and 2.5g carbon additive, for which significantly improved charge duration and discharge energy was observed, compared to the standard cathode. Based on long-term cycling results in a life test, a battery life of 5500 cycles was projected for this new cathode composition (end-of-life: 80% of the initial capacity of the state-of-the-art composition). Considering the wide capacity window of 5-100% SOC, 38 Ah applied in the life test, this suggest the feasibility of a design life of 7000 cycles.

In the following, we discuss the project results with respect to the quantitative performance parameters defined as project targets (**Table 5**). As Na-$NiCl_2$ batteries are assembled in the discharged state, their area-specific **cell capacity** corresponds directly to the cathode loading. In this project, we applied high cathode loadings of **~150 mAh/cm^2** in both planar and tubular cells, which is very important for the cost-efficiency of Na-$NiCl_2$ batteries.

The **energy density on cell level** is a nominal quantity, which is calculated from the nominal cell capacity, nominal cell voltage, and cell weight. Due to the early stage of planar cell development, we did not implement new cathode formulations in planar prototype and pilot cells in this project, but focused on demonstrating their performance with state-of-the-art nickel/iron cathodes. In terms of cell weight, we conclude that transfer from a tubular to a planar cell geometry generally results in an increase in weight (and volume). This is because relevant passive cell components scale with the circumference of the active cell area (e.g. α-alumina insulator, seals, cell housing). While adoption of alternative cell materials and/or the stacking of cells could compensate this, further investigations would be required to assure safe operation and long cycle life. Thus, we do not consider the planar cell design to enhance the energy density on cell level at the current stage of development. Nevertheless, we employed enhanced cathode formulations with increased specific capacity in tubular cell modules. Long-term cycling (>5 months, 260 cycles) was demonstrated for compositions with up to 20% nickel reduction (e.g. -25 g Ni + 2.5 carbon, **174 mAh/g, 0.4 Ah/g Ni**). Thus, the target of 160 Wh/kg nominal energy density on cell level was almost achieved.

Table 5 Performance of (i) planar cells with standard cathode and (ii) tubular cells with enhanced cathode.

	project targets	planar cell with standard cathode	tubular cell with enhanced cathode
cell capacity	150 mAh/cm^2	☑	☑
nominal energy density on cell level*	160 Wh/kg		
↳ specific cathode capacity	180 mAh/g	(not investigated)	(☑) 174 mAh/g
↳ ratio of capacity to mass of Ni	0.4 Ah/g	(not investigated)	0.4 Ah/g
↳ and/or reduction of cell weight	-80 g	☒	(not investigated)
nominal discharge rate	C/2, 75 mA/cm^2	☑ 80 mA/cm^2	(☑) 50 mA/cm^2
max. discharge rate (30 s pulse)	1.5C, 225 mA/cm^2	(not investigated)	☑ 230 mA/cm^2
charge duration, 10-90% SOC	5 h	☑	☒
charge duration, 10-100% SOC	8 h	☑	☒
projected service life	7000 cycles	☒	(☑) 6700 cycles

In terms of **nominal discharge rate** and **charge duration**, we demonstrated planar cells with standard sodium-nickel chloride cathode to provide stable discharge at a rate of >C/2 (**80 mA/cm^2**), while meeting the project targets for **charge duration** (<5 h for 10-90% SOC, <8 h for 10-100% SOC). To improve comparability of our studies with literature reports, we did not demonstrate discharge pulses at 1.5C in these experiments.

The life test procedure applied to tubular cell modules focused on a nominal discharge rate of C/3, **50 mA/cm^2**, as this represents realistic conditions for this battery type. Discharge pulses at 1.5C (230 mA/cm^2) and 1C (150 mA/cm^2) were successfully applied in each life cycle. Cycling was performed over a wide capacity window of 38 Ah (5-100% SOC), with charge times amounting to ~12h for the standard cathode, and ~10.5 h for enhanced cathode formulations. Based on these measured values, the tubular cell modules with enhanced cathode formulation do not yet meet the original targets for charge time of 5 h and 8 h at lower SOC windows. Nevertheless, their performance in terms of charge time, discharge energy, and cycle life is significantly improved, compared to state-of-the-art tubular cells. During the life test, the best new cathode formulation provides an initial discharge energy of ~390 Wh/kg (with respect to the cathode mass), compared to 350 Wh/kg for the standard cathode. Considering 280 Wh/kg as end-of-life criterion, the standard cathode is projected to provide a **service life** of ~3900 life cycles, while the enhanced formulation can achieve **~5500 life cycles**.

For the planar cell developed in this project, such a high cycle life is currently not within reach. Nevertheless, our prototype cells demonstrated the highest number of cycles (>140 cycles at 50 mAh/cm^2 cathode loading, >50 cycles at 150 mAh/cm^2) and the highest cumulative capacity (> 7 Ah/cm^2) reported for planar Na-$NiCl_2$ cells so far. On pilot cell level, geometrical variations and dimensional tolerances of the cell components, in particular of sintered ceramic parts, presently hinder precise fittings, efficient management of molten materials, and hermetic sealing. Further work on pilot cell development is ongoing also beyond this project.

From a company's perspective, FZSoNick is open to evaluate the possibility of introducing a production line for planar cells in the future. On cell level, planar components are more compatible with automated high-volume manufacturing and quality control routines, decreasing production costs. This applies not only to the load-bearing Na-β”-alumina electrolyte, but also to other cell components like electrodes, interfacial coatings, shims, and current collectors. Planar geometries cost-effectively accommodate changes of components (e.g. amount of electrode material), so that cells can be adapted and optimized

for different applications (such as power density, energy density, lifetime, weight/ volume, operation temperature, etc.). At a battery level, the assembly of planar cells facilitates interconnection, reduces packaging costs, and adds flexibility and scalability to the battery design. Introduction of short stacks with bipolar plates may further reduce internal resistances, weight, and complexity. However, further development of planar cells with industrially relevant specifications is required to demonstrate that planar cells can compete with other commercial energy storage solutions. Presently, FZSONICK is evaluating the potential markets for both tubular and planar cells for the next 5 years (supported by an external partner). This includes energy storage (especially for residential and industrial solar application), back-up for power utilities, and back-up for oil and gas applications. Furthermore, FZSoNick's commitment in investigating a planar cell design is continued in the SOLSTICE project, where FZSONICK is present as industrial partner, supporting EMPA in testing planar cells with new Zn based cathodic materials.

Thus, overall, the HiPerSonick consortium achieved the overarching project goals in time. This is despite a difficult working environment during the COVID-19 pandemic, which imposed home office regulations, restricted experimental and production activities to respect physical distancing and hygiene rules, and which lead to numerous delivery delays from suppliers. Furthermore, the economic circumstances led to a substantial reduction in incoming orders at FZSoNick.

Until now, the HiPerSoNick project led to the publication of 8 scientific papers in peer-reviewed scientific journals, and to the submission of 1 invited scientific book chapter. At least 5 more manuscripts are currently in preparation. The results were and are further brought to a wider audience in 32 conference contributions. At Empa and EPFL, 1 BSc thesis, 1 MSc thesis, and 1 PhD thesis were successfully completed within the project. Furthermore, 2 PhD students and 6 postdoctoral researcher were educated, most of which are employed now by Swiss companies in the energy sector.

5 Outlook and next steps

Our developments on both planar and tubular Na-$NiCl_2$ cells over the past four years of the HiPerSoNick project have demonstrated the values and limitations of both geometries for high-temperature batteries.

In the short term, FZSoNick is planning to implement the newly developed cathode formulations with reduced nickel content in the production of their batteries, starting at the beginning of 2023. As shown in this project, the new cathode formulations provide enhanced cycle stability, compared to state-of-the-art cathodes, while reducing cell cost and cell weight.

In terms of a planar cell design, our implementations show several advantages of this geometry, which can accommodate cathodes of variable composition, packing density, and thickness, allowing to tune the ratio of delivered power to stored energy of the cell. Scaled to planar pilot cells, we demonstrated cell cycling results of a first technological implementation of this cell design at industrially relevant high areal capacity. However, for cost-efficient production, further developments are required, e.g. to improve the design and processing of planar high-temperature cells, both in terms of cell performance, cell weight/volume, reliability, and cost effectiveness. Furthermore, operation of large planar cells has not been demonstrated outside the glovebox so far. Thus, for commercial sodium-nickel chloride batteries with large active area, transition from a tubular towards a planar cell design requires further developments.

Nevertheless, we continue to employ the unique competences on high-temperature sodium-nickel chloride cells developed in this project. Both FZSoNick and Empa are part of the EU Horizon 2020 project "Sodium-zinc molten-salt batteries for low-cost stationary storage (SOLSTICE)", financed with 7.7 M€ from 2021-2024 (consortium of 11 partners, https://www.solstice-battery.eu/). Here, planar cell experiments are applied to screen new cathode compositions and to study the influence of cathode microstructure and composition on cycling performance, while long-term cycling is performed on selected compositions in tubular cell modules.

6 National and international cooperation

Follow-up project; Sodium-zinc molten salt batteries for low-cost stationary storage (SOLSTICE), H2020 research and innovation action, H2020-LC-BAT-8-2020. Coordinator Helmholtz-Zentrum Dresden, partners Empa and FZSoNick, 01/2021 – 12/2024, https://www.solstice-battery.eu.

Demonstrator unit; a 68 kWh molten salt battery (FZSoNick, state-of-the-art tubular sodium-nickel chloride cells) is in use at Empa's post-fossil mobility demonstrator "move", https://www.empa.ch/web/move/elektromobilitat.

Project granted; Battery2030+, https://battery2030.eu/, H2020 coordination and support action, H2020-LC-BAT-12-2020. Coordinator Uppsala University, partner Empa. 09/2021 – 08/2023.

European Technology and Innovation Platform Batteries Europe, Empa member of working group 1 since 12/2019

European Research Institute Alistore, https://alistore.eu/, Empa elected member since 06/2021

Battery European Partnership Association, https://www.bepassociation.eu/, Empa founding member since 12/2021

Swiss Battery Association iBAT, https://ibat.swiss/association/, Empa founding member and elected executive committee member, since 12/2021

PhD Thesis, Daniel Alexander Landmann, Design guidelines for next-generation sodium-nickel-chloride batteries. École Polytechnique Fédérale de Lausanne (EPFL), successful defense 07.12.2021, nominated for EPFL Doctorate Award 2023.

PhD Thesis, Marie-Claude Bay, Na-β”-alumina ceramic electrolytes for fast-charging next-generation sodium-ion batteries. Albert-Ludwigs Universität Freiburg, successful defense 18.06.2020.

Student exchange with Prof. Jeff Sakamoto's group, Michigan University, USA. (Marie-Claude Bay, 3 months, 2019).

Master Thesis, Isabel Streicher, Charge transport in the porous cathode of sodium-nickel-chloride batteries. Albert-Ludwigs Universität Freiburg, Deutschland (10/2019).

Bachelor Thesis, Jan Roman Seitz, Fabrication of zirconia-toughened alumina composites. ETH Zürich, Switzerland (08/2018).

7 Communication

Technical newspaper articles

Benedikt Vogel, BFE-Forschung: Wie Schweizer Fachhochschulen, Hochschulen und Universitäten die Batterie neu erfinden, 22.06.2022, https://www.ee-news.ch/de/article/48894/bfe-forschung-wie-schweizer-fachhochschulen-hochschulen-und-universitaten-die-batterie-neu-erfinden.

Organisation of Venues

Swiss Battery Days 2022, Dübendorf, swissbatterydays.empa.ch, jointly with PSI and BFH, Empa scientific committee member and main organizer, 29.-31.08.2022

2nd Swiss Battery Association iBAT conference, Biel, ibat.swiss/ibat-2nd-annual-conference/, Biel, Empa co-organizer, 30.11.2021

Battery 2030+/European Lithium Institute Green Battery Conference, ONLINE, www.green-battery-conference.eu, Empa symposium co-organizer, 5./12./19./26.10.2021

Battery cell manufacturing – the role of Swiss industry, ONLINE, https://ibat.swiss/battery-cell-manufacturing-the-role-of-swiss-industry/, Empa workshop organizer, 29.09.2021

ACS Fall Meeting 2021, acs.org, ONLINE, Empa symposium co-organizer, 23.08.2021

Swiss Battery Days 2020/21, ONLINE, https://indico.psi.ch/event/8700/ , jointly with PSI and BFH, Empa scientific committee member, 15.-17.02.2021

International Sodium Battery Symposium jointly with Fraunhofer IKTS, ONLINE, idw-online.de/en/event66017, Empa scientific committee member, 13.-14.01.2021

Swiss Battery Days 2019, Dübendorf, swissbatterydays.empa.ch, jointly with PSI and BFH, Empa scientific committee member and main organizer, 26.-28.08.2019

Presentations at Conferences

C. Battaglia et al., Elucidating the Rate-Limiting Processes in High-Temperature Sodium-Metal Chloride Batteries, **242nd ECS Meeting**, **2022**/10, Atlanta, USA *(accepted)*.

T. Lan et al., Planar Sodium-Nickel Chloride Cells with 150 mAh cm^{-2} Areal Capacity, 73rd Annual Meeting of the International Society of Electrochemistry, **2022**/09, online *(accepted)*.

N. Kovalska, M. Heinz, C. Battaglia, T. Graule, G. Blugan Swiss Battery Days 2022, Planar Na-b" -Al_2O_3 solid electrolytes. Swiss Battery Days **2022**/08, Dübendorf, *(planned)*.

N. Kovalska, M. Heinz, C. Battaglia, T. Graule, G. Blugan, Tape casting and die pressing of large flat Na-b"-Al2O3 solid electrolytes for planar Na-Batteries, Shaping 8, **2022**/09, Dübendorf, *(accepted)*.

M. V. F. Heinz et al., Current developments in sodium-metal chloride (ZEBRA) batteries. **Sodium (Na) Battery Symposium SBS-3**, **2022**/09, Berlin, Germany **(invited***, planned***)**.

M. V. F. Heinz et al., Application of metal-anodes at ambient and high temperatures. **46th International Conference & Exposition on Advanced Ceramics & Composites (ICACC2022**), **2022**/01, Daytona Beach, USA **(invited**, online**)**.

M. V. F. Heinz, D. Landmann, G. Graeber, D. Landmann, M.-C. Bay, E. Svaluto-Ferro, T. Lan, L. Sieuw, C. Battaglia; Cell and cathode design for sodium-metal chloride batteries. **Molten Salts**, **2021**/12, International Virtual Academy, online.

C. Battaglia et al., Alternative electrolytes for sodium-ion batteries. **90. International Workshop on Sodium-Ion Batteries** organized by the European Commission, **2021**/11, Alava, Spain (**invited**, online).

M. V. F. Heinz, D. Landmann, G. Graeber, D. Landmann, M.-C. Bay, E. Svaluto-Ferro, T. Lan, L. Sieuw, C. Battaglia; High-power cathodes for sodium-metal chloride batteries. ***Green Batteries***, **2021**/10, Würzburg/online.

M. V. F. Heinz, G. Graeber, D. Landmann, M.-C. Bay, E. Svaluto-Ferro, T. Lan, L. Sieuw, C. Battaglia; Advanced cathode design for sodium-metal chloride batteries. **Euromat**, **2021**/09, Virtual Conference, online. *Highlight Talk.*

M. V. F. Heinz; Innovative Materialsysteme und keramische Werkstoffe für Batterieanwendungen. Schweizerischer Verband für Materialwissenschaft und Technologie, **Tag der Werkstoffe 2021** "Hochleistungskeramiken", 2021/05/15, ONLINE*. Invited presentation.*

D. Landmann, G. Graeber, M. V. F. Heinz, C. Battaglia; Design guidelines for next-generation sodium-nickel chloride batteries. **MRS Spring Meeting**, 18.-23.04.2021, ONLINE. *Presentation.*

C. Battaglia et al., Electrolytes for next-generation lithium and sodium batteries. **80. Technical University Delft Seminar**, **2021**/02, Delft, Netherlands (**invited**, online).

M. V. F. Heinz, M.-C. Bay, D. Landmann, G. Graeber, R. Grissa, C. Battaglia; Solid-state vs. liquid-state application of metal anodes. **Swiss Battery Days**, 15.-17.02.2021, ONLINE. *Presentation.*

D. Landmann, G. Graeber, M. V. F. Heinz, C. Battaglia; Sodium stripping and plating from Na-β"-alumina ceramics beyond 1000 mA/cm^2. **Swiss Battery Days**, 15.-17.02.2021, ONLINE. *Poster presentation.*

M. V. F. Heinz, G. Graeber, D. Landmann, C. Battaglia; Pressure management and cell design in solid-electrolyte batteries, at the example of a sodium-nickel chloride battery. **International Sodium Battery Symposium**, 13.-14.01.2020, ONLINE. *Presentation.*

M. V. F. Heinz, M.-C. Bay, D. Landmann, G. Graeber, R. Grissa, C. Battaglia; Sodium stripping and plating from Na-β″-alumina ceramics: solid-state vs. liquid-state application. **International Sodium Battery Symposium**, 13.-14.01.2020, ONLINE. *Presentation.*

D. Landmann, G. Graeber, M. V. F. Heinz, C. Battaglia; Sodium stripping and plating from Na-β"-alumina ceramics beyond 1000 mA/cm^2. **International Sodium Battery Symposium**, 13.-14.01.2020, ONLINE. *Poster presentation.*

D. Landmann, G. Graeber, M. V. F. Heinz, S. Haussener, C. Battaglia; Sodium plating and stripping from Na-β''-alumina ceramics beyond 1000 mA/cm^2. **MRS Fall Meeting**, 28.11.-04.12.2020, ONLINE. *Presentation,* ***Best Presentation Award and Science as Art Competition Finalist.***

C. Battaglia; Interface stability in all-solid-state batteries. **Battery 2030+ virtual webinar**, 18.05.2020, *ONLINE, ~1000 attendees, invited presentation.*

M. V. F. Heinz; Innovative Materialsysteme und keramische Werkstoffe für Batterieanwendungen. Schweizerischer Verband für Materialwissenschaft und Technologie, **Tag der Werkstoffe 2020** "Hochleistungskeramiken", 23.04.2020, Empa Dübendorf. *Cancelled due to COVID19, invited presentation.*

D. Landmann, G. Graeber, M. V. F. Heinz, S. Haussener, C. Battaglia, Sodium plating and stripping from Na-β''-alumina ceramics beyond 1000 mA/cm^2. **ECS PRIME**, 04.-09.10.2020, ONLINE. *Presentation.*

M. V. F. Heinz, G. Graeber, D. Landmann, C. Battaglia; Pressure management and cell design in solid-electrolyte batteries, at the example of a sodium-nickel chloride battery. **E-MRS Fall Meeting**, 14.-17.09.2020, Warsaw, Poland. ***Cancelled*** *due to COVID19.*

M.-C. Bay, M. Wang, R. Grissa, M. V. F. Heinz, J. Sakamoto, C. Battaglia, Sodium Plating from Na-β″-Alumina Ceramics at Room Temperature, Paving the Way for Fast-Charging All-Solid-State Batteries. **E-MRS Fall Meeting**, 14.-17.09.2020, Warsaw, Poland. ***Cancelled*** *due to COVID19.*

D. Landmann, M. V. F. Heinz, S. Haussener, C. Battaglia, Design guidelines for next-generation sodium-metal-halide batteries. **MODVAL17**,12.-13.3.2020, Sion. ***Postponed*** *to 2021 due to COVID19.*

M.-C. Bay, M. V. F. Heinz, U. F. Vogt, C. Battaglia; Impact of liquid phase formation on microstructure and conductivity of Li-stabilized Na-β''-alumina ceramics. **2019 MRS Fall Meeting**, 01.-06.12.2019, Boston, Massachusetts. *Presentation.*

C. Battaglia et al., Impact of liquid phase formation on microstructure and conductivity of Li-stabilized Na-β''-alumina ceramics. **71. Materials Research Society (MRS) Fall Meeting**, **2019**/11, Boston, USA.

M.-C. Bay, M. V. F. Heinz, R. Figi, C. Schreiner, U. F. Vogt, C. Battaglia, Impact of liquid phase formation on microstructure and conductivity of Li-stabilized Na-β''-alumina ceramics. **2nd Swiss and Surrounding Battery Days**, 26.-28.08.2019, Empa Academy, Dübendorf. *Presentation.*

D. Landmann, M. V. F. Heinz, S. Haussener, C. Battaglia, Design guidelines for next-generation sodium-metal-halide batteries. **2nd Swiss and Surrounding Battery Days**, 26.-28.08.2019, Empa Academy, Dübendorf. *Poster.*

D. Landmann, M. V. F. Heinz, S. Haussener, C. Battaglia, Design guidelines for next-generation sodium-metal-halide batteries. **NRG 2019: Energy Systems: managing the transition to renewables**, 10-14.06.2019, Champéry. *Poster.*

D. Landmann, M. V. F. Heinz, S. Haussener, C. Battaglia, Design guidelines for next-generation sodium-metal-halide batteries. **Empa PhD Student's Symposium**, 26.11.2018, Empa Dübendorf. *Poster, awarded* ***Poster Presentation Award****.*

D. Landmann, M. V. F. Heinz, C. Battaglia, Multi Physics Modeling of Molten Salt Batteries, **2. ZEBRA Meeting**, 18.-19.10.2018, Meiringen*. Presentation.*

G. Blugan, S. C. Ligon, T. Graule, Tape Casting as Technology in ZEBRA Battery Manufacturing, **2. ZEBRA Meeting**, 18.-19.10.2018, Meiringen*. Presentation.*

M. V. F. Heinz, M.-C. Bay, U.F. Vogt, C. Battaglia, Grain size effects on activation energy & conductivity of β''-alumina electrolytes. **2. ZEBRA Meeting**, 18.-19.10.2018, Meiringen, Switzerland. *Presentation.*

8 Publications

[Gutierrez2022] R. Gutierrez, T. Lan, M. V. F. Heinz, C. Battaglia, S. Haussener, "Solar molten salt batteries: Feasibility and analysis", manuscript available upon request, **2022**.

[Kovalska2022b] N. Kovalska, G. Blugan, M. V. F. Heinz, D. Basso, C. Battaglia, T. Graule, "Glass sealing of a-alumina-to-metal", manuscript available upon request, **2022**.

[Kovalska2022a] N. Kovalska, G. Blugan, M. V. F. Heinz, D. Basso, C. Battaglia, T. Graule, "Tape casting and die pressing of large flat Na-b"-Al_2O_3 solid electrolytes for planar Na-Batteries", manuscript available upon request, **2022**.

[Lan2022b] T. Lan, E. Svaluto-Ferro, N. Kovalska, G. Graeber, L. Sieuw, D. Landmann, F. Vagliani, D. Basso, A. Turconi, G. Blugan, T. Graule, C. Battaglia, M. V. F. Heinz*, "Scaling of planar sodium-metal chloride battery cells to 90 cm^2 active area", manuscript available upon request, **2022**.

[Lan2022a] T. Lan, G. Graeber, L. Sieuw, D. Landmann, E. Svaluto-Ferro, F. Vagliani, D. Basso, A. Turconi, C. Battaglia, M. V. F. Heinz*, "Planar sodium-metal chloride batteries with high cathode loading", manuscript available upon request, **2022**.

[Heinz2022] M. V. F. Heinz, D. Landmann, D. Basso, C. Battaglia, Chapter 6.9: "Sodium Nickel Chloride (ZEBRA) batteries", Elsevier, Treatise on process metallurgy, Vol. 2 (invited, manuscript available upon request), **2022**.

[Landmann2022] D. Landmann, E. Svaluto-Ferro, M. V. F. Heinz*, P. Schmutz, C. Battaglia, "Elucidating the rate-limiting processes in high-temperature sodium-metal chloride batteries". ***Adv. Science***, vol. 9, p.2201019, **2022**.

[Landmann2022PhD] D. A. Landmann, "Design guidelines for next-generation sodium-nickel-chloride batteries". ***EPFL PhD thesis*** No. 9537, **2022**.

[Graeber2021] G. Graeber, D. Landmann, E. Svaluto-Ferro, F. Vagliani, D. Basso, A. Turconi, M. V. F. Heinz*, C. Battaglia; "High-performance, planar sodium-metal chloride batteries enabled by a mixed iron / nickel cathode", ***Adv. Funct. Mater.***, vol. 31, p. 2106367, **2021**.

[*Heinz2021*] M. V. F. Heinz*, M.-C. Bay, U. F. Vogt, C. Battaglia, "Grain size effects on activation energy and conductivity of ion conductors with highly resistive grain boundaries, shown exemplarily for Na-β''-Al_2O_3 ceramics". ***Acta Materialia***, vol. 213, p.116940, **2021**.

[Bay2021] M.-C. Bay, M. V. F. Heinz*, U. F. Vogt, C. Battaglia; "Analysis of c-lattice parameters to evaluate Na_2O loss from and Na_2O content in β''-alumina ceramics". ***Ceramics International***, vol 47, p.13402, **2021**.

[*Landmann2020*] D. Landmann, G. Graeber, M. V. F. Heinz*, S. Haussener, C. Battaglia; "Sodium plating and stripping from Na-β''-alumina ceramics beyond 1000 mA/cm^2". ***Mater. Today Energy***, vol 18, p. 100515, **2020**.

[*Heinz2020*] M. V. F. Heinz*, G. Graeber, D. Landmann, C. Battaglia; "Pressure management and cell design in solid-electrolyte batteries, at the example of a sodium—nickel chloride battery", ***J. Power Sources***, vol. 465, p. 228268, **2020**.

[*Ligon2020b*] S. C. Ligon*, M.-C. Bay, M. V. F. Heinz, C. Battaglia, T. Graule, and G. Blugan, "Large planar Na-β''-Al_2O_3 solid electrolytes for next generation Na-batteries", ***Materials***, vol. 13, no. 2, p. 433, **2020**.

[*Ligon2020a*] S. C. Ligon*, G. Blugan, M.-C. Bay, C. Battaglia, M. V. F. Heinz, and T. Graule, "Performance analysis of Na-Na-β''-alumina"-Al_2O_3/YSZ solid electrolytes produced by conventional sintering and by vapor conversion of α-Al_2O_3/YSZ", ***Solid State Ionics***, vol. 345, p. 115169, **2020**.

[*Bay2020*] # M.-C. Bay, M. V. F. Heinz*, C. Linte, A. German, G. Blugan, C. Battaglia, U. F. Vogt, "Impact of sintering conditions and zirconia addition on flexural strength and ion conductivity of Na-β"-alumina ceramics", ***Mater. Today Commun.***, p. 101118, **2020**.

[*Bay2019*] # M.-C. Bay, M. V. F. Heinz*, R. Figi, C. Schreiner, D. Basso, N. Zanon, U. F. Vogt, and C. Battaglia, "Impact of liquid phase formation on microstructure and conductivity of Li-stabilized Na-β''-alumina ceramics", ***ACS Appl. Energy Mater.***, vol. 2, no. 1, p. 687, **2019**.

*corresponding author

within Innosuisse project Sonibat

9 References

[1] N. Weber, J. T. Kummer, *Annu. Power Sources Conf.* **1967**, *21*, 37.

[2] P. T. Moseley, in *Sodium Sulfur Batter.* (Eds.: J.L. Sudworth, A.R. Tilley), Hall, Chapman And, **1985**, pp. 17–76.

[3] J. Coetzer, M. M. Thackeray, **1978**.

[4] C. H. Dustmann, *J. Power Sources* **1998**, *72*, 27.

[5] R. C. Galloway, S. Haslam, *J. Power Sources* **1999**, *80*, 164.

[6] J. L. Sudworth, *J. Power Sources* **2001**, *100*, 149.

[7] C. H. Dustmann, *J. Power Sources* **2004**, *127*, 85.

[8] R. Benato, N. Cosciani, G. Crugnola, S. Dambone Sessa, G. Lodi, C. Parmeggiani, M. Todeschini, *J. Power Sources* **2015**, *293*, 127.

[9] S. Restello, N. Zanon, E. Paolin, in *INTELEC, Int. Telecommun. Energy Conf.*, **2013**, pp. 1–5.

[10] D. Larcher, J. M. Tarascon, *Nat. Chem.* **2015**, *7*, 19.

[11] J. Prakash, L. Redey, D. R. Vissers, *J. Power Sources* **2000**, *87*, 195.

[12] O. Veneri, C. Capasso, S. Patalano, *Appl. Energy* **2017**, *185*, 2005.

[13] F. Bignucolo, M. Coppo, G. Crugnola, A. Savio, *Energies* **2017**, *10*, 1497.

[14] S. Bracco, F. Delfino, A. Trucco, S. Zin, *J. Power Sources* **2018**, *399*, 372.

[15] N. Shamim, E. C. Thomsen, V. V. Viswanathan, D. M. Reed, V. L. Sprenkle, G. Li, *Materials (Basel).* **2021**, *14*, DOI 10.3390/ma14092280.

[16] J. St. John, *Greentechmedia* **2015**, *Jan 22*, date accessed 2021/09/21.

[17] H. Viccaro, *Dly. Gaz.* **2015**, *Nov 13*, date accessed 2021/09/21.

[18] Chilwee, *www.chilweebattery.com/durathon-battery/sodium-nickel-chloride-battery.html* **2022**, date accessed 2022/06/03.

[19] Alumina Battery Systems, *https://alumina.systems/battery-systems/* **2022**, date accessed 2022/06/03.

[20] R. Wagner, N. Preschitschek, S. Passerini, J. Leker, M. Winter, *J. Appl. Electrochem.* **2013**, *43*, 481.

[21] K. B. Hueso, M. Armand, T. Rojo, *Energy Environ. Sci.* **2013**, *6*, 734.

[22] European Commission, *Communication* **2020**, *COM(2020)4*, 1.

[23] R. C. Galloway, *J. Electrochem. Soc.* **1987**, *134*, 256.

[24] S. Restello, G. Lodi, E. Paolin, in *INTELEC, Int. Telecommun. Energy Conf.*, **2011**, pp. 1–6.

[25] H. Böhm, in *Handb. Batter. Mater. Second Ed.*, John Wiley \& Sons, Ltd, **2011**, pp. 719–756.

[26] B. Dunn, H. Kamath, J. M. Tarascon, *Science (80-.).* **2011**, *334*, 928.

[27] S. Ma, M. Jiang, P. Tao, C. Song, J. Wu, J. Wang, T. Deng, W. Shang, *Prog. Nat. Sci. Mater. Int.* **2018**, *28*, 653.

[28] G. L. Soloveichik, *Annu. Rev. Chem. Biomol. Eng.* **2011**, *2*, 503.

[29] M. Sufyan, N. A. Rahim, M. M. Aman, C. K. Tan, S. R. S. Raihan, *J. Renew. Sustain. Energy*

2019, *11*, 14105.

[30] FZSoNick, *Download From Fzsonick.Com/Home* **2021**, *08/31*, 7.

[31] C. H. Dustmann, *J. Power Sources* **2004**, *127*, 85.

[32] X. Zhan, M. M. Li, J. M. Weller, V. L. Sprenkle, G. Li, *Materials (Basel).* **2021**, *14*, DOI 10.3390/ma14123260.

[33] H. J. Chang, X. Lu, J. F. Bonnett, N. L. Canfield, S. Son, Y. C. Park, K. Jung, V. L. Sprenkle, G. Li, *J. Power Sources* **2017**, *348*, 150.

[34] G. Li, X. Lu, J. Y. Kim, K. D. Meinhardt, H. J. Chang, N. L. Canfield, V. L. Sprenkle, *Nat. Commun.* **2016**, *7*, 10683.

[35] G. Li, X. Lu, J. Y. Kim, J. P. Lemmon, V. L. Sprenkle, *J. Mater. Chem. A* **2013**, *1*, 14935.

[36] X. Lu, G. Li, J. Y. Kim, J. P. Lemmon, V. L. Sprenkle, Z. Yang, *J. Power Sources* **2012**, *215*, 288.

[37] A. Manthiram, *ACS Cent. Sci.* **2017**, *3*, 1063.

[38] M. J. Lain, J. Brandon, E. Kendrick, *Batteries* **2019**, *5*, DOI 10.3390/batteries5040064.

[39] R. Benato, S. D. Sessa, G. Crugnola, M. Todeschini, S. Zin, *2015 AEIT Int. Annu. Conf. AEIT 2015* **2015**, IEEE Italy Sec.

[40] P. Albertus, S. Babinec, S. Litzelman, A. Newman, *Nat. Energy* **2018**, *3*, 16.

[41] X. Lu, H. J. Chang, J. F. Bonnett, N. L. Canfield, K. Jung, V. L. Sprenkle, G. Li, *J. Power Sources* **2017**, *365*, 456.

[42] R. Christin, Multiphysics Modeling of Sodium Nickel Chloride Cells, Grenoble Alpes University, **2015**.

[43] R. Weidl, M. Schulz, M. Hofacker, H. Dohndorf, M. Stelter, *AIP Conf. Proc.* **2016**, *1765*, UNSP 020004.